Remote Sensing of Environment 140 (2014) 60–77

Contents lists available at ScienceDirect

Remote Sensing of Environment

journal homepage: www.elsevier.com/locate/rse

Evaluation of MODIS albedo product (MCD43A) over grassland, agriculture and forest surface types during dormant and snow-covered periods

Zhuosen Wang [a,*], Crystal B. Schaaf [a], Alan H. Strahler [b], Mark J. Chopping [c], Miguel O. Román [d], Yanmin Shuai [e,f], Curtis E. Woodcock [b], David Y. Hollinger [g], David R. Fitzjarrald [h]

[a] Environmental, Earth, and Ocean Sciences Department, University of Massachusetts Boston, Boston, MA USA
[b] Center for Remote Sensing, Department of Geography and Environment, Boston University, Boston, MA, USA
[c] Department of Earth and Environmental Studies, Montclair State University, Montclair, NJ, USA
[d] Terrestrial Information Systems Laboratory (Code 619), NASA Goddard Space Flight Center, Greenbelt, MD, USA
[e] Earth Resources Technology Inc., Laurel, MD, USA
[f] NASA Goddard Space Flight Center, Greenbelt, MD, USA
[g] USDA Forest Service Northern Research Station, Durham, NH, USA
[h] Atmospheric Sciences Research Center, University at Albany, SUNY, Albany, NY, USA

ARTICLE INFO

Article history:
Received 25 October 2012
Received in revised form 14 August 2013
Accepted 17 August 2013
Available online 19 September 2013

Keywords:
MODIS standard and daily albedo product
Snow albedo
Forest
Grassland
Spatial representativeness

ABSTRACT

This study assesses the Moderate-resolution Imaging Spectroradiometer (MODIS) BRDF/albedo 8 day standard product and products from the daily Direct Broadcast BRDF/albedo algorithm, and shows that these products agree well with ground-based albedo measurements during the more difficult periods of vegetation dormancy and snow cover. Cropland, grassland, deciduous and coniferous forests are considered. Using an integrated validation strategy, analyses of the representativeness of the surface heterogeneity under both dormant and snow-covered situations are performed to decide whether direct comparisons between ground measurements and 500-m satellite observations can be made or whether finer spatial resolution airborne or spaceborne data are required to scale the results at each location. Landsat Enhanced Thematic Mapper Plus (ETM+) data are used to generate finer scale representations of albedo at each location to fully link ground data with satellite data. In general, results indicate the root mean square errors (RMSEs) are less than 0.030 over spatially representative sites of agriculture/grassland during the dormant periods and less than 0.050 during the snow-covered periods for MCD43A albedo products. For forest, the RMSEs are less than 0.020 during the dormant period and 0.025 during the snow-covered periods. However, a daily retrieval strategy is necessary to capture ephemeral snow events or rapidly changing situations such as the spring snow melt.

1. Introduction

Surface albedo, defined as the ratio of the total (hemispheric) reflected solar radiation flux to the incident flux upon the surface, quantifies the radiation interaction between the atmosphere and the land surface. It plays a crucial role in land surface climate and biosphere models (Dickinson & Hanson, 1984; Dirmeyer & Shukla, 1994; Lofgren, 1995). Carbon-only accounting approaches which ignore the albedo impacts of forests can significantly overestimate the climatic benefit of offsets (Thompson, Adams, & Johnson, 2009). As a key land physical parameter controlling the surface radiation energy budget, an absolute accuracy of 0.02–0.05 is required by climate models for global surface albedo (Dickinson, 1983, 1995; Dickinson et al., 2008; Henderson-Sellers & Wilson, 1983).

The surface reflectivity changes significantly with the appearance of snow. Snow also alters the exchange of moisture between the surface and the atmosphere especially during the snowmelt period (Marshall, Roads, & Glatzmaier, 1994). The snow albedo contributes a strong positive feedback in surface modeling studies (Betts & Ball, 1997; Bonan, Chapin, & Thompson, 1995; Gardner & Sharp, 2010; Koltzow, 2007; Li, Sun, Wang, & Liu, 2009; Molders, Luijting, & Sassen, 2008; Pedersen, Godtliebsen, & Roesch, 2008; Pedersen, Roeckner, Luthje, & Winther, 2009, Qu & Hall, 2006; Rutter et al., 2009; Thomas & Rowntree, 1992; Viterbo & Betts, 1999; Wyser et al., 2007). The albedo at local solar noon for snow-covered forests is usually less than 0.3 in the shortwave, but it can reach 0.57 or higher for snow-covered grassland and barren locations (Jin et al., 2002).

The Moderate-resolution Imaging Spectroradiometer (MODIS) BRDF/albedo products (Schaaf, Wang, & Strahler, 2011a, Schaaf et al., 2002, 2008) have been available since 2000 and provide high quality surface reflectance anisotropy retrievals over a variety of land surface

* Corresponding author. Tel.: +1 617 287 5029.
E-mail address: wangzhuosen@gmail.com (Z. Wang).

0034-4257/$ – see front matter © 2013 Elsevier Inc. All rights reserved.
http://dx.doi.org/10.1016/j.rse.2013.08.025

types (Jin et al., 2003b; Liang et al., 2002; Liu et al., 2009; Román et al., 2009, 2010). The Bidirectional Reflectance Distribution Function (BRDF) models and shapes (Gao, Schaaf, Strahler, Jin, & Li, 2003; Hill, Averill, Jiao, Schaaf, & Armston, 2008) are also increasingly being used to provide information about the surface vegetation structure and the albedo quantities have been embraced by the global climate modeling and numerical assimilation communities (Dickinson et al., 2008; Fang et al., 2007; Lawrence & Chase, 2007; Morcrette, Barker, Cole, Iacono, & Pincus, 2008; Myhre, Kvalevag, & Schaaf, 2005, Oleson et al., 2003; Roesch, Schaaf, & Gao, 2004; Tian et al., 2004; Wei et al., 2001; Zhou et al., 2003).

Although reported on a 500 m grid, the MODIS BRDF/albedo products are usually retrieved utilizing observations from a larger area depending on the view angles. The footprint of observations increases with the increase in the scanning angle (Tan et al., 2006; Wolfe, Roy, & Vermote, 1998). Observations are weighted by angular coverage before the retrieval but it must still be acknowledged that the 500 m gridded product actually represents information from a larger area.

A number of studies have validated the MODIS albedo product by a direct "point-to-pixel" comparison (Chen, Liang, Wang, Kim, & Martonchik, 2008; Liu et al., 2009; Salomon, Schaaf, Strahler, Gao, & Jin, 2006; Wang et al., 2004) with the assumption that both the tower and satellite albedo roughly sample the same spatial domain. However, ground measurements from tower usually only cover a limited area, which is much smaller than the MODIS spatial resolution. An important difficulty encountered whenever attempts are made to compare satellite-retrieved albedo values to tower-measured albedo data is that the footprint of the ground measurement is not always representative of the greater satellite footprint. This is particularly true of rapidly changing surface conditions during senescence, green-up, and varying periods of snow cover. Assessments of spatial representativeness using Landsat data can provide an estimate of the general ability of the satellite retrievals to capture the tower measurements (Román et al., 2009, 2010). However, conditions can change so rapidly during dormancy and ephemeral snow events that such assessments must be reconsidered frequently for each situation.

Initial investigations with "point-to-pixel" comparisons at the AmeriFlux Canadian University of California-Irvine (UCI) burn forest sites in Canada suggest that the MODIS winter values were usually lower than the tower values (Román et al., 2009). However these locations represent field sites with high spatial heterogeneity during winter periods. To consider the spatial scaling effect, finer spatial resolution Landsat Enhanced Thematic Mapper Plus (ETM+) data have been usually used to validate MODIS BRDF/albedo products (Fang, Liang, Chen, Walthall, & Daughtry, 2004; Jin et al., 2003b; Liang et al., 2002; Susaki, Yasuoka, Kajiwara, Honda, & Hara, 2007). Barnsley et al. (2000) and Lucht, Hyman, et al. (2000) used Landsat data to analyze the spatial scaling effect on the albedo of a semi-desert environment prior to the launch of MODIS. It must be noted however that most of these studies have assumed a Lambertian surface to estimate Landsat albedo although Jin et al. (2003b) calculated a Landsat albedo by applying the ratio of the MODIS hemispherical albedo at local solar noon to the directional surface reflectance at the Landsat observing geometry.

While the MODIS BRDF/albedo products have been evaluated during the growing season for a number of vegetated land covers with high accuracy (Disney, Lewis, Thackrah, Quaife, & Barnsley, 2004; Jin et al., 2003a, 2003b; Knobelspiesse, Cairns, Schmid, Román, & Schaaf, 2008; Liang et al., 2002; Liu et al., 2009; Lyons, Jin, & Randerson, 2008; Roesch et al., 2004; Román et al., 2009, 2010; Salomon et al., 2006; Samain et al., 2008; Shuai, Schaaf, Strahler, Liu, & Jiao, 2008; Stone, Anderson, Shettle, Andrews, & Loukachine, 2008; Susaki et al., 2007; Wang, Barlage, Zeng, Dickinson, & Schaaf, 2005; Wang et al., 2004), the assessment of the results during dormant and snow-covered seasons (Román et al., 2009, 2010; Schaaf, Liu, Gao, & Strahler, 2011b; Wang et al., 2012) has only just begun.

The spatial patterns of albedo will change seasonally if the surface is comprised of different land types. This is especially true during dormant periods (when vegetation is not photosynthetically active and leaves are either brown and/or very few). Jin et al. (2002) analyzed the effect of snow over different land covers and showed that snow caused high heterogeneity in the surface albedo making validation more difficult. Therefore, differences between the tower measurements and MODIS albedo should be expected and any evaluation of the MODIS BRDF/albedo products over dormant seasons, both snow-covered and snow-free, needs to pay particular attention to spatial scaling effects.

For agricultural and temperate grassland areas, the ground is often covered by dense uniform vegetation during the growing season. Thus, the surface is relative homogenous and ground measurements match well with MODIS products (Chen et al., 2008; Jin et al., 2003b; Liang et al., 2002; Liu et al., 2009; Román et al., 2009, 2010; Susaki et al., 2007). However, these surfaces are often considerably more heterogeneous during dormant or partly snow-covered periods. Jin et al. (2003b) and Chen et al. (2008) showed that there are relatively large differences between ground albedos and MODIS albedo products during these seasons.

Modeling and monitoring the albedo of forests during the snow-covered periods can be difficult. A snow-covered forest in winter is made up an upper layer of dark leaves and branches and a lower layer of bright snow on the forest floor. Because of the upper foliage in dense evergreen forests, the reflected photons from the snow surface have difficulties escaping the forest canopy especially under high zenith viewing angles; moreover, a large fraction of the understory may be shaded in winter scenes, owing to the higher solar zenith angles. However, the reflectance from deciduous forests, where snow information is more visible through a canopy of bare branches, is relatively high. The density of the canopy can also affect whether a pixel is designated as snow-covered or snow-free.

This study aims to assess the accuracy of MODIS albedo products by comparison with ground measurements after establishing the spatial representativeness of vegetated surfaces during dormant and snow-covered situations. Section 2 describes both the ground measurements and MODIS albedo products and Section 3 outlines the assessment strategy. In Section 4, we compare the ground measurements to MODIS albedos and Landsat albedos where appropriate and discuss the overall accuracy of MODIS products during the dormant and snow-covered seasons.

2. Datasets

2.1. Ground measurements

The primary validation sites used for the MODIS Albedo product have historically been the Surface Radiation Budget Network (SURFRAD) sites (Augustine, DeLuisi, & Long, 2000) which are maintained in the United States by NOAA as part of the Baseline Surface Radiation Network (BSRN) (Ohmura et al., 1998). The World Climate Research Programme (WCRP) Radiative Fluxes Working Group initiated the BSRN to support the research projects of the WCRP and other scientific programs. These seven SURFRAD sites (Fort Peck, MT, Sioux Falls, SD, Penn State, PA, Bondville, IL, Table Mountain, CO, Goodwin Creek, MS and Desert Rock, NV) (Table 1) are used again in this study. In addition to the seven SURFRAD sites, the Boulder, CO site is also another BSRN site close to the Table Mountain site that utilizes pyranometers mounted on a 300 m tower. These eight sites provide the highest quality intercalibrated albedo measurements.

Three additional sites of New England forests from the AmeriFlux network are also used in this study. AmeriFlux was established by the Department of Energy (DOE) in 1996 to provide continuous observations of ecosystem level exchanges of CO_2, water, and energy, including surface albedo (Law et al., 2002; Running et al., 1999).

Table 1
SURFRAD, BSRN, and AmeriFlux ground sites.

Station name	Latitude/longitude	Tower height/footprint (m)	State	Land cover	MODIS tile	Network
Boulder	40.05/−105.01	300/3788.25	Colorado	Grassland	H09V04	BSRN
Fort Peck	48.31/−105.10	10/126.28	Montana	Grassland	H11V04	SURFRAD
Goodwin Creek	34.25/−89.87	10/126.28	Mississippi	Grassland	H10V05	SURFRAD
Sioux Falls	43.73/−96.62	10/126.28	South Dakota	Grassland	H11V04	SURFRAD
Table Mountain	10/126.28	Colorado	Grassland	H09V04	SURFRAD	
40.13/−105.24						
Desert Rock	36.62/−116.02	10/126.28	Nevada	Desert, sparse grass	H08V05	SURFRAD
Bondville	40.05/−88.37	10/126.28	Illinois	Agriculture	H11V04	SURFRAD
Penn State	40.72/−77.93	10/126.28	Pennsylvania	Agriculture	H12V04	SURFRAD
Harvard EMS	42.538/−72.172	30/366	Massachusetts	Mixed forest	H12V04	AmeriFlux
Howland Larch	45.216/−68.709	30/366	Maine	Deciduous needleleaf forest	H13V04	AmeriFlux
Howland West	45.209/−68.747	30/366	Maine	Evergreen needleleaf forest	H13V04	AmeriFlux

Total downward and upward radiation (0.28–3.0 μm) is measured by Eppley pyranometers mounted on the 10 m towers at the SURFRAD sites while the Boulder site utilizes a 300 m tower. Normal Incidence Pyranometers and shaded pyranometers are used to measure the direct normal and diffuse shortwave fluxes (Augustine et al., 2000). The instruments are ventilated and heated during the winter so that there is a great deal of confidence in the winter measurements as well as the growing season ones. Kipp and Zonen albedometers in the shortwave (0.3–2.8 μm) are used to measure albedo at AmeriFlux sites. These albedometers are mounted on 30 m towers and not routinely heated and ventilated, therefore the data are not considered as reliable during snow precipitation periods. Ground albedo is calculated by the ratio of upwelling radiation and downwelling radiation during the local mid-day time. The footprints of 10 m, 30 m, and 300 m towers are estimated to be about 126 m, 366 m and 3788 m in diameter respectively.

$$f = 2H\tan(\mathrm{HFOV}^{\circ}) \quad (1)$$

where f is the circular footprint of ground tower measurements, H [m] is the tower height, and HFOV [degrees] is its half of field of view. HFOV is 81° (Michalsky, Harrison, & Berkheiser, 1995).

The Bondville SURFRAD site is located southwest of Champaign, Illinois, in an agricultural region (Fig. 1). This site represents a mixture of crops and drainage ditches which are maintained with a variety of harvesting and fallowing practices. It is quite heterogeneous at the MODIS scale (Liu et al., 2009; Salomon et al., 2006). The Sioux Falls SURFRAD site is located on the grounds of the Earth Resources Observation and Science (EROS) Data Center, South Dakota, and is covered by grass. The Goodwin Creek site, west of Oxford, Mississippi, is located on rural pasture land surrounded by deciduous trees. The Penn State University (PSU) SURFRAD site is located on the grounds of PSU's agricultural research farm about 6 miles southwest of State College, Pennsylvania and is in a broad Appalachian valley between the Tussey and Bald Eagle Ridges. The Fort Peck SURFRAD station is located on the Fort Peck Tribes Reservation in Montana. This site is dominated by native grasses. The Table Mountain SURFRAD station is located in Colorado and is a mix of exposed rocks, sparse grasses, desert shrubs and small cactus. The Boulder BSRN station, also in Colorado, is very close to the Table Mountain station and is covered by grass. The Desert Rock SURFRAD station is covered with very sparse vegetation and lies to the northwest of Las Vegas, Nevada. The AmeriFlux site at Howland Forest is located in central Maine, U.S.A., about 35 miles north of Bangor. The natural stands in this boreal–northern hardwood transitional forest consist of hemlock–spruce–fir, and hemlock–hardwood mixtures. The evergreen needle-leaf canopy height at Howland West Tower is about 20 m. The albedo data used here are from 2007 to 2009, and the albedometer was heated during the winter of 2009. The Howland Larch Tower is surrounded by deciduous needle-leaf trees (larch, *Larix laricina*) (Hollinger, Ollinger, Richardson, Meyers, & Dail, 2010). The albedo data were collected in 2008 for the Larch Tower. The AmeriFlux Harvard Environmental Measurement Station (EMS) tower at Harvard Forest lies in the central Massachusetts town of Petersham. The dominant species include red oak, red maple, black birch, white pine, and hemlock.

2.2. Satellite albedo

2.2.1. MCD43A standard BRDF/albedo product

The standard MODIS BRDF/albedo product (MCD43A) (Lucht, Schaaf, & Strahler, 2000; Schaaf et al., 2002) provides the weighting parameters associated with the RossThick-LiSparse Reciprocal (RTLSR) BRDF model that describes the reflectance anisotropy of each pixel at a 500-m gridded resolution. Both a sufficient number of observations and good angular sampling are needed to achieve a full inversion retrieval and estimate a high quality BRDF. Acknowledged as a tradeoff between the temporal stability of the surface reflectance and the availability of sufficient angular samples, a 16-day period of cloud-free, atmospherically-corrected surface reflectances from both Terra (MOD) and Aqua (MYD) is used to derive MCD43A BRDF/albedo (Gao, Schaaf, Strahler, & Lucht, 2001; Roy, Lewis, Schaaf, Devadiga, & Boschetti, 2006; Wanner et al., 1997). With an 8 day system of overlapping processing, more phenological variability can be accurately characterized. A backup algorithm (also called a magnitude inversion) is employed if a high quality full inversion retrieval cannot be accomplished due to poor angular sampling or insufficient input observations (Schaaf et al., 2002). This a priori knowledge method often performs quite well under normal situations (Jin et al., 2003a, 2003b; Liu et al., 2009; Salomon et al., 2006) but should be considered a poor quality result and is assigned a poor quality flag. The MCD43A BRDF/albedo standard product only retrieves a snow albedo quantity when the majority of observations during a 16 day period are snow-covered. Snow-covered and non-snow observations are currently always processed separately.

The intrinsic black-sky albedo (BSA) at local solar noon and the white-sky albedo (WSA) is generated by integrating the BRDF calculated from the three retrieved parameters (f_{iso}, f_{geo} and f_{vol}). Blue sky albedo, which considers both the diffuse and direct incident radiation for a specific time and atmospheric state, can be calculated as follows (Lewis & Barnsley, 1994):

$$\alpha_{\text{blue-sky}}(\theta_i) = \mathrm{SKYL}(\theta_i)\alpha_{\text{white-sky}} + (1-\mathrm{SKYL}(\theta_i))\alpha_{\text{black-sky}}(\theta_i) \quad (2)$$

where $\mathrm{SKYL}(\theta_i)$ is the proportion of diffuse irradiation at a certain solar zenith angle θ_i. The SKYL is measured by the shaded pyranometer at the SURFRAD and Howland Forest (West and Larch) sites. Harvard EMS Forest does not have ground SKYL data and the MODIS aerosol product (MOD08) is used to calculate the proportion of diffuse irradiation.

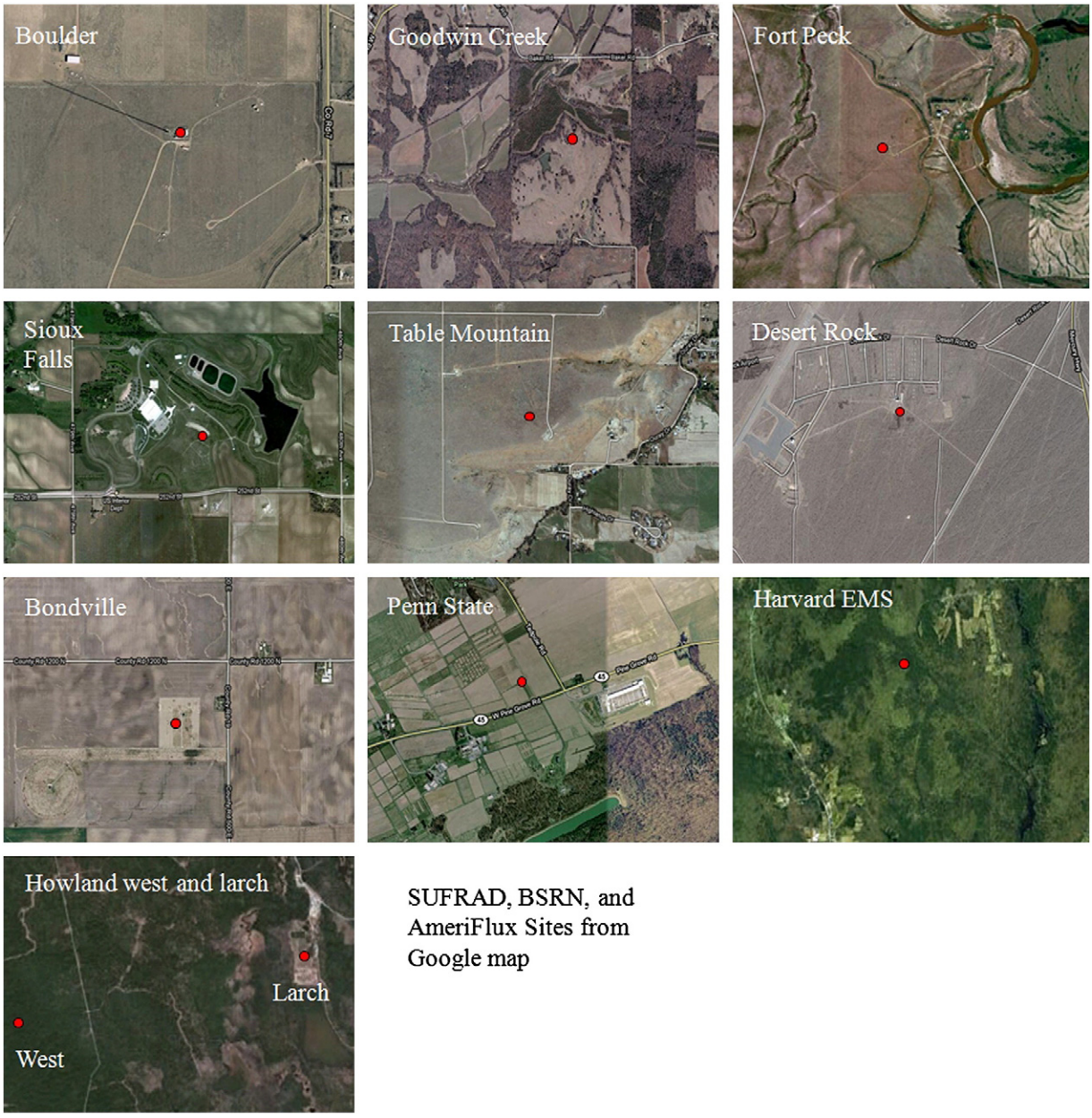

Fig. 1. The locations of the eleven SUFRAD, BSRN and AmeriFlux sites — Boulder, Goodwin Creek, Fort Peck, Sioux Falls, Table Mountain, Desert Rock, Bondville, Penn State, Harvard EMS, Howland West and Howland Larch sites from Google map.

In addition to the spectral quantities, three broadband albedos of VIS (0.3–0.7 μm), NIR (0.7–5.0 μm) and shortwave (0.3–5.0 μm) are calculated from the 7 spectral bands via narrow to broadband conversion coefficients (Liang, Strahler, & Walthall, 1999; Stroeve et al., 2005).

$$\alpha_{\text{shortwave,snowfree}} = 0.3973\alpha_1 + 0.2382\alpha_2 + 0.3489\alpha_3 - 0.2655\alpha_4 + 0.1604\alpha_5 - 0.0138\alpha_6 + 0.0682\alpha_7 + 0.0036 \quad (3)$$

$$\alpha_{\text{shortwave,snow}} = 0.1574\alpha_1 + 0.2789\alpha_2 + 0.3829\alpha_3 + 0.1131\alpha_5 + 0.0694\alpha_7 - 0.0093. \quad (4)$$

2.2.2. MCD43A direct broadcast (DB) albedo data

The MODIS DB BRDF/albedo product (Shuai, 2010) which is utilized for regional applications (e.g., forest, agriculture and disturbance monitoring) is operated in a daily rolling mode to provide more frequent surface Nadir BRDF-Adjusted Reflectances (NBAR) and albedos than the current standard product. Two versions of the DB mode are utilized in this study. First, the 16-day daily mode uses 16 days worth of reflectances as input but weights the more recent clear observations (with the highest observation coverage) more heavily. A retrieval is attempted each day based on the proceeding 16 days' worth of data. Full inversions are performed if there are sufficient high quality and well sampled angular observations, where the quality of the angular sampling is determined by reference to the Weights of Determination (Lucht & Lewis, 2000). Otherwise a magnitude inversion will be processed with the a priori backup database being updated with the most recent full inversion results. Second, the 1-day daily mode, a magnitude inversion is performed each day using the full inversions from the 16-day daily mode as the a priori information for each succeeding day. While this mode emphasizes the single day observation the most heavily, it is also more sensitive to any cloud contamination or residual aerosols affecting that single look.

2.2.3. Landsat data

Landsat ETM+ data at 30 m spatial resolution are available from United States Geological Survey (USGS), and the Landsat Ecosystem Disturbance Adaptive Processing System (LEDAPS) (Masek et al., 2006) is used to convert low level Digital Number (DN) values to Top-of-Atmosphere (TOA) radiance and then to surface reflectance by atmospheric correction using the Second Simulation of the Satellite Signal in the Solar Spectrum (6S) radiative transfer code (Kotchenova, Vermote, Matarrese, & Klemm, 2006; Vermote et al., 1997). Shortwave reflectance is generated via the narrowband to broadband coefficients for Landsat data (Liang, 2001):

$$r_{\text{shortwave}} = 0.356r_1 + 0.130r_3 + 0.373r_4 + 0.085r_5 + 0.072r_7 - 0.0018 \quad (5)$$

where $r_{\text{shortwave}}$ is shortwave reflectance and r_i are the spectral Landsat reflectances.

An unsupervised classification is performed on the Landsat surface reflectances over a tower site. Instead of assuming Lambertian surfaces, the Landsat albedo is calculated from an Anisotropic Reflectance Factor (ARF) taken at a location nearby where a pure high quality MODIS pixel associated with that same land cover class is available (Shuai, Masek, Gao, & Schaaf, 2011).

3. Methodology

3.1. Assessment strategy

As stated earlier, the footprints of the 10 m and 30 m tower albedometers are about 126 m and 366 m diameter respectively, which is much smaller than a 500-m gridded MODIS pixel. Therefore, we use a validation method based on finer spatial resolution satellite data (usually Landsat) to consider the spatial representativeness of the tower observation footprint as compared to the MODIS pixel (Fig. 2). While it is reasonable to compare ground measurements to MODIS 500 m grid products if the tower measurements are spatially representative, it is not appropriate to directly compare values if the ground measurements are not homogeneous or spatially representative of larger areas (Román et al., 2009). Therefore, once the 30 m Landsat albedos have been reconstructed over the more heterogeneous surfaces, the Landsat albedos are compared first to field measurements and then averaged to various different spatial resolutions to evaluate the coarser resolution MODIS albedo products.

3.2. Spatial representativeness

The semivariogram (Carroll & Cressie, 1996; Davis, 1986; Isaaks & Srivastava, 1989; Matheron, 1963) is one of the most efficient tools for describing spatial representativeness. The characteristics of semivariograms (e.g., sill, range, and nugget effect) can reveal the spatial variability of land surfaces and reveal the scaling effects associated with remotely sensed data (Woodcock, Strahler, & Jupp, 1988a, 1988b; Román et al., 2009, 2010).

Here, we estimate semivariograms from the 30-m spatial resolution Landsat ETM+ surface reflectances at different periods of the year to check the spatial representativeness of the region around the ground tower area.

$$\gamma_E(h) = 0.5 \cdot \frac{\sum_{i=1}^{N(h)} (z_{xi} - z_{xi+h})^2}{N(h)} \quad (6)$$

where $\gamma_E(h)$ is the variogram estimator between reflectances that are within certain distance; z_{xi} is the surface reflectance at pixel location x; z_{xi+h} is the surface reflectance of another pixel within a lag distance h, and $N(h)$ is the number of paired data at a distance of h.

The spatial attributes (range, sill and nugget effect) can then be modified to fit a spherical model (Matheron, 1963) to the variogram estimator:

$$\gamma_{sph}(h) = \begin{cases} c_0 + c \cdot \left(1.5 \cdot \frac{h}{a} - 0.5\left(\frac{h}{a}\right)^3\right) & \text{for } 0 \le h \le a \\ c_0 + c & \text{for } h > a \end{cases} \quad (7)$$

where a, which describes the average patch size of the landscape (Cooper, Barmuta, Sarnelle, Kratz, & Diehl, 1997), is the distance that there is no further correlation of biophysical property associated with a point. The sill (c) describing the maximum semivariance is the ordinate value of the range at which the variogram levels off to an asymptote. The nugget effect (c_0) describes the value when the variogram does not reach zero variance at $h = 0$. It depends on the variance associated with small scale variability, measurement errors, or a combination of these (Noreus, Nyborg, & Hayling, 1997).

There are gaps (Scan Line Corrector (SLC)-off) in Landsat ETM+ images after May 31, 2003 because of the failure of SLC. We treated the SLC-off part as fill values and excluded them in the processing.

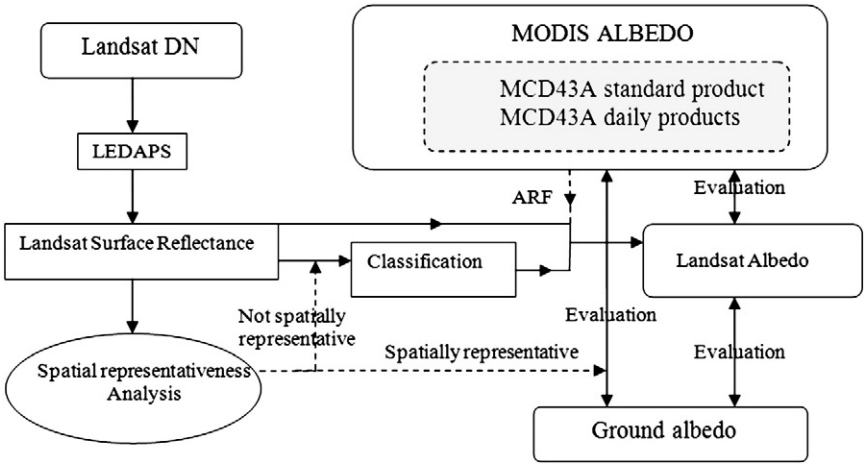

Fig. 2. Flow chart of MODIS albedo validation as compared to ground data and albedos reconstructed from the finer scale Landsat data.

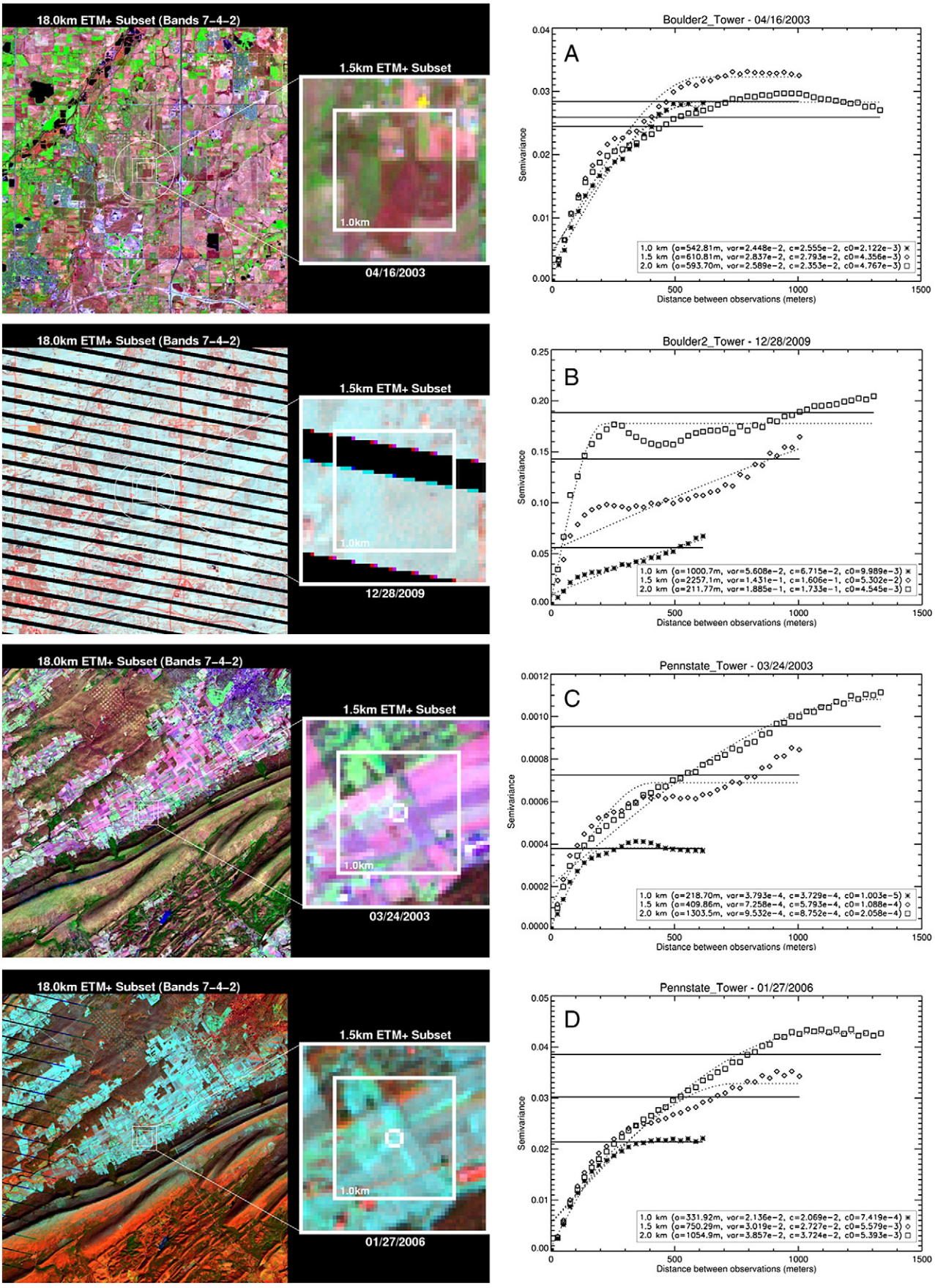

Fig. 3. Top-of-Atmosphere (TOA) shortwave reflectance composite (ETM+ Bands 7–4–2) and corresponding semivariogram functions, variogram estimator (points), spherical model (dotted curves), and sample variance (solid straight lines) using regions of 1.0 km (asterisks), 1.5 km (diamonds), and 2.0 km (squares), centered over Boulder on 4/16/2003 (A), Boulder on 12/28/2009 (B), Penn State on 03/24/2003 (C) and Penn State on 01/27/2006 (D). The circle stands for the tower footprint and the black strips are caused by SLC-off.

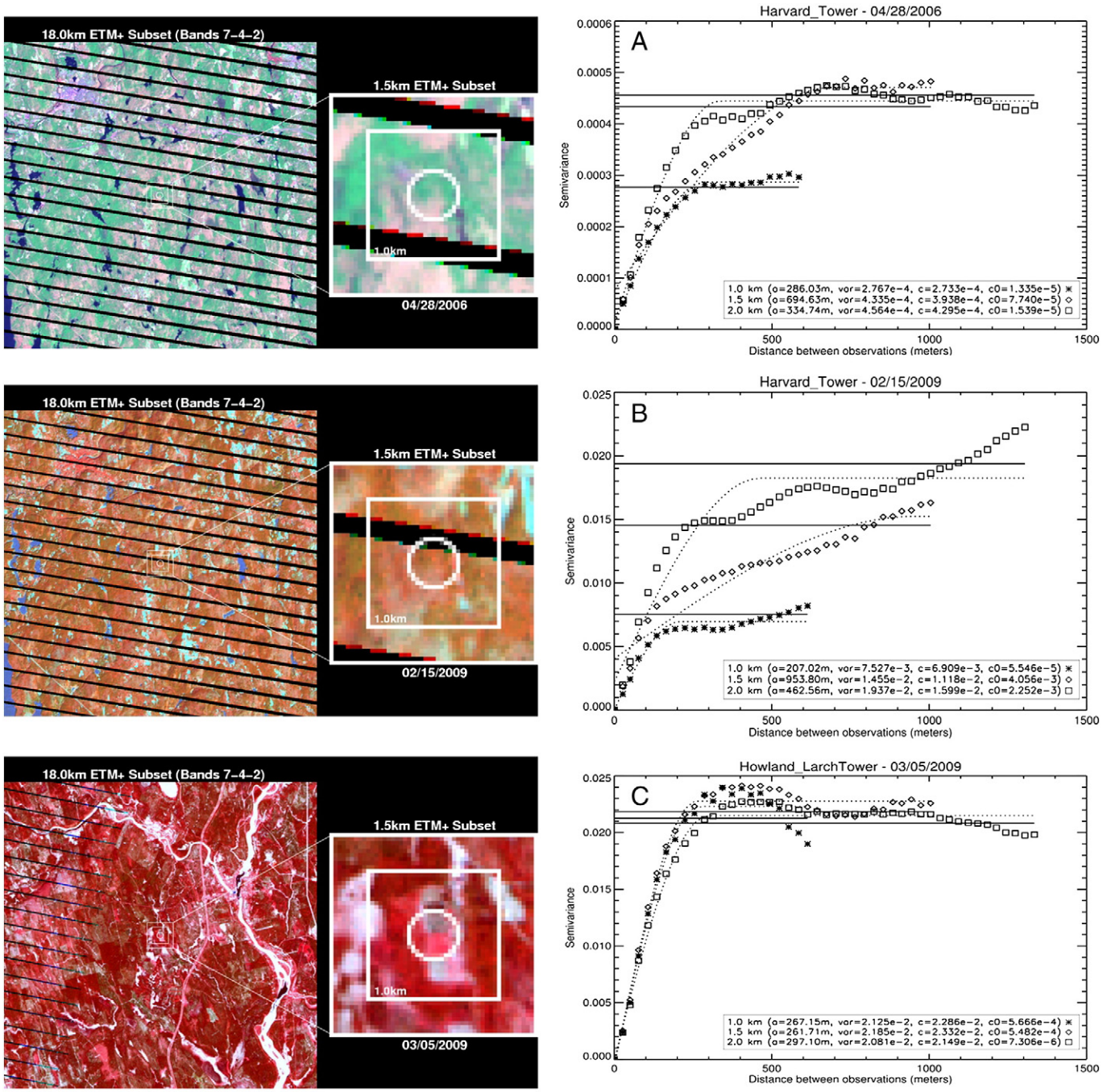

Fig. 4. Top-of-Atmosphere (TOA) shortwave reflectance composite (ETM+ Bands 7–4–2) and corresponding semivariogram functions, variogram estimator (points), spherical model (dotted curves), and sample variance (solid straight lines) using regions of 1.0 km (asterisks), 1.5 km (diamonds), and 2.0 km (squares), centered over Harvard EMS on 04/28/2006 (A), 02/15/2009 (B), and Howland Larch on 03/05/2009 (C). The circle stands for the tower footprint and the black strips are caused by SLC-off.

3.3. Comparison of ground albedo with Landsat and MODIS albedo

The ground albedos were first compared to MODIS albedos directly (point–pixel comparison). The ground albedos, Landsat and MODIS albedos were then compared at different spatial scales. Clear sky Landsat ETM+ data were collected during the dormant and snow-covered periods from year 2003 to 2009 for SURFRAD/BSRN sites. Landsat data were first aggregated to 4 × 4 (120 m), which is similar to the 10 m tower footprints (except for the Boulder site with its 300 m tower), to check the consistency of Landsat albedo with ground measurements. It is important to recognize that MODIS 500 m observations may come from footprints two to four times larger if the view zenith angles are very large (although it must also be noted these data are also weighted by their observation coverage before they are gridded to a 500 m spatial resolution). Therefore Landsat albedo values were aggregated by 17 × 17 pixels (to 510 m), 33 × 33 pixels (to 990 m), 49 × 49 pixels (to 1470 m) and 65 × 65 pixels (to 1950 m) for comparison with the MODIS scale albedos.

4. Results and discussions

4.1. Spatial representativeness analysis

Land cover is relatively homogeneous over an extended region at the Fort Peck, Table Mountain, Boulder and Desert Rock sites (and the tower sites are spatially representative of the satellite pixels), but the

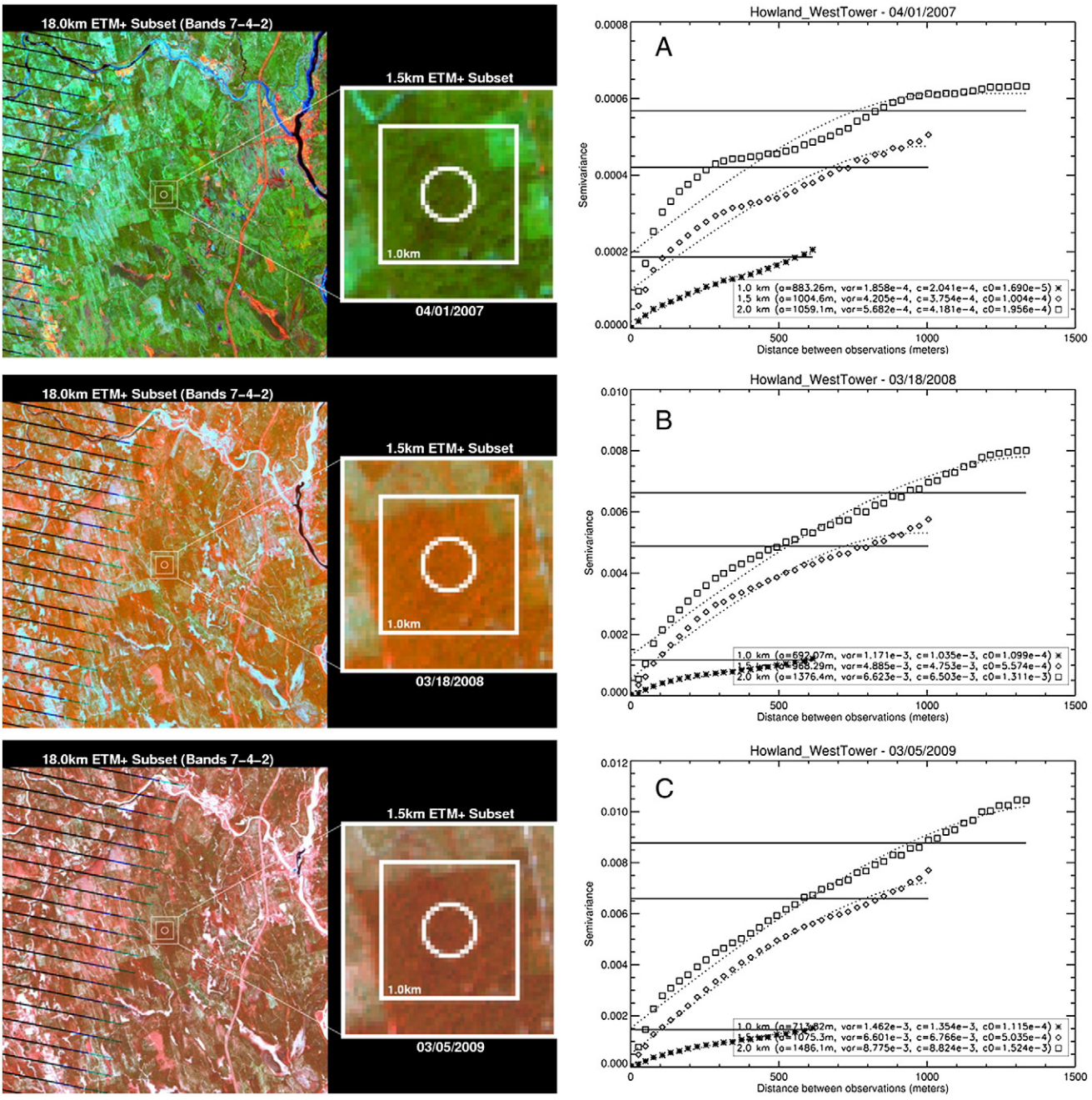

Fig. 5. Top-of-Atmosphere (TOA) shortwave reflectance composite (ETM+ Bands 7–4–2) and corresponding semivariogram functions, variogram estimator (points), spherical model (dotted curves), and sample variance (solid straight lines) using regions of 1.0 km (asterisks), 1.5 km (diamonds), and 2.0 km (squares), centered over Howland West on 04/01/2007 (A), 03/18/2008 (B), and on 03/05/2009 (C). The circle stands for the tower footprint and the black strips are caused by SLC-off.

Bondville, Goodwin Creek, Sioux Falls and Penn State sites are more spatially complex and heterogeneous during both the dormant and snow-covered seasons.

Smaller sill values indicate a more homogenous surface for which the ground measurements are more spatially representative. During the dormant period, Boulder is relatively homogenous (Fig. 3A). The ranges of the three spatial scales (1.0 km, 1.5 km, and 2.0 km) are nearly the same and the sill values are very close. During the partly snow-covered period (Fig. 3B), not all of the area is covered by snow. The sill values increase as larger statistical areas are considered and the sills are larger than those computed during dormant period. The Penn State station is located on agricultural land, but there is forest land to the south very close to the tower. The sill values increase when even more forest land at the larger subsets is included. During the snow period, the agricultural land is dominated by a bright surface snow, while over forest land, most of the information is from darker upper layer of the trees since the snow only exists on the floor of the forest and is mostly obscured by needleleaf foliage or trunks and branches. So with an increase in the statistical area, not only does the sill increase but the range increases as well. For grass/agriculture sites that are also surrounded by forests, it can be more heterogeneous at the MODIS scale even when it may be relatively homogenous over the tower footprint.

The Howland West Tower site is surrounded by a dense evergreen needleleaf forest. Trees to the east and west of West Tower have been harvested prior to 2007 and part of these cut areas are within 1 km of the site. Trees to the north of the West Tower were cut before 03/18/2008 and an extensive area of trees to the north of the West Tower

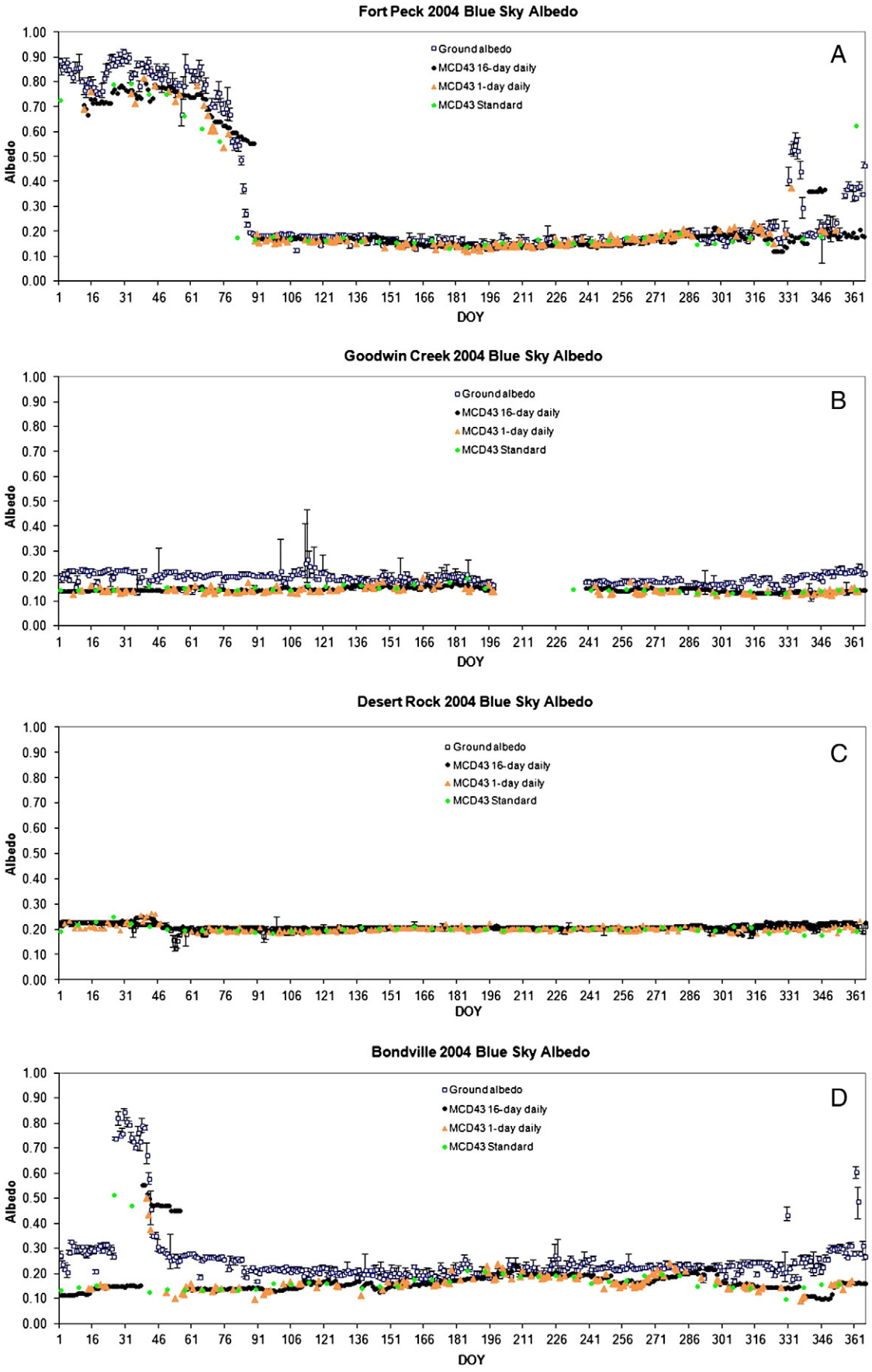

Fig. 6. Comparison of temporal shortwave albedo for Fort Peck (A), Goodwin Creek (B), Desert Rock (C) and Bondville (D) sites in 2004, Harvard EMS site in 2007 (E) and Howland West site in 2007 (F) and 2008 (G).

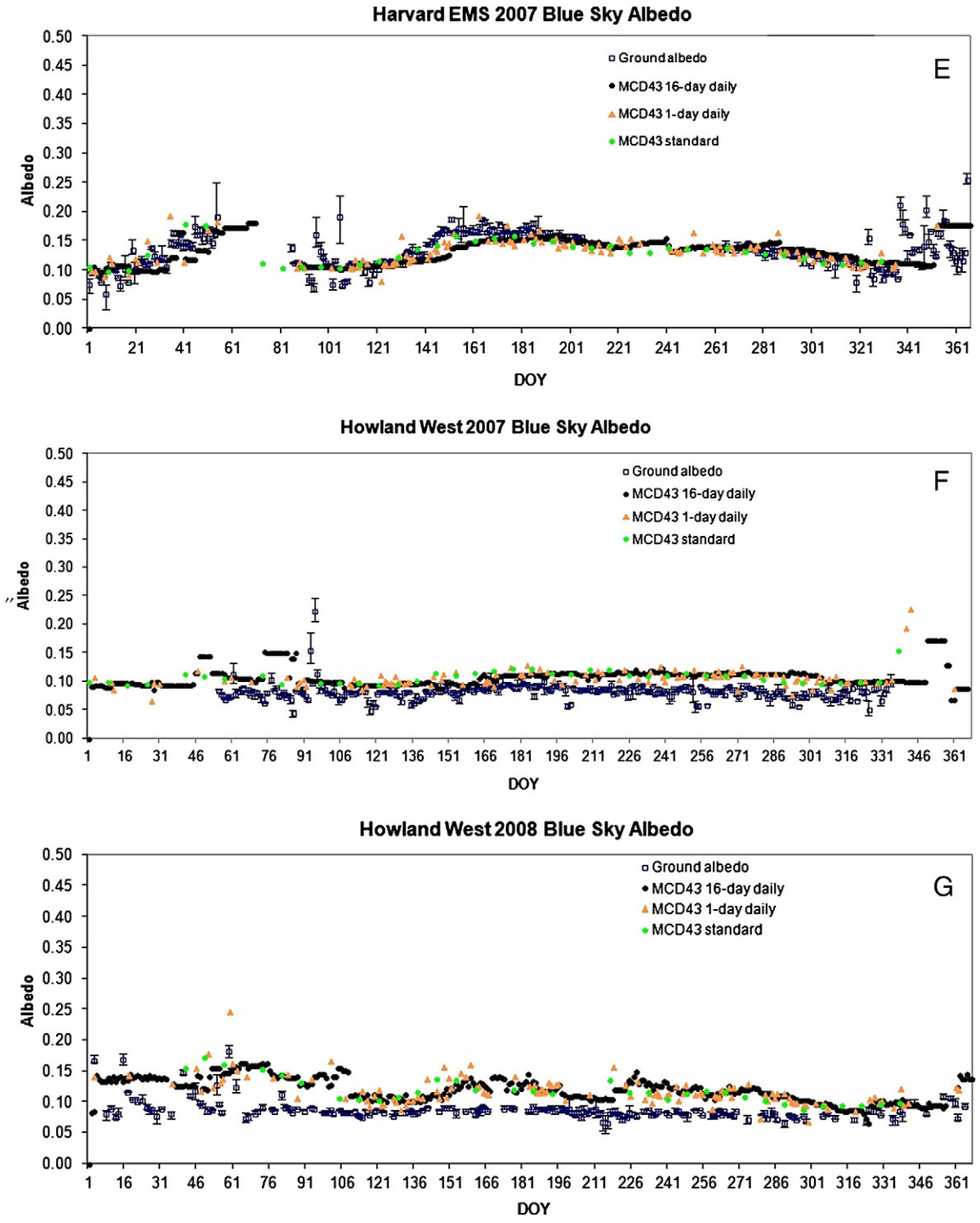

Fig. 6 (*continued*).

was cut before 03/05/2009. The semivariograms of the Howland West Tower site shows that sill values for the 1.0 km area, which only include relatively small amounts of the recently cut areas, are very low during all three years (Fig. 5). However, when considering a 2.0 km statistical area around the tower in 2007, the sill value is at a minimum of 0.0006 and then increases to 0.008 in 2008 and larger than 0.01 in 2009. Therefore the cut areas surrounding the West Tower result in larger discrepancies in the sill values at the larger statistical areas. The Howland Larch site is located in a small area of larch trees and surrounded by evergreen forest. The sill is much larger than the Howland West site (Fig. 4C) although the sill and range values are very close for all 3 spatial scales (1.0 km, 1.5 km and 2.0 km). A mixture of deciduous and evergreen forest surrounds the Harvard EMS tower. There are some bare areas in the vicinity, and the sill values are relatively large when this bare area is covered by bright snow during the snow-covered period (Fig. 4B). The Harvard EMS site is relatively spatially representative during the dormant snow-free period however (Fig. 4A).

4.2. Comparison of albedo

4.2.1. Comparison between ground albedo and MODIS albedo

The MCD43A standard and 16-day daily albedos are relatively stable because they make use of all of the clear sky observations in 16 days. By

convention the standard product is named with the first day of the 16 day period (and uses that solar zenith angle) while the 16-day daily product is named with the last day of 16-day period and uses that solar zenith angle because the observations from latest days are emphasized with higher weights. Therefore the MCD43A standard albedos suggest a decrease a few days earlier than the actual melt period while the 16-day daily albedo show the more correct delayed decreasing trend (e.g., at Sioux Falls and Bondville sites). Note that both the MCD43A standard and 16-day daily products use the majority situation during the period to decide whether to retrieve a snow or snow-free albedo. The MCD43A 1-day daily products however are based on the single day determination of whether an observation is snow-covered or not (via the snow flag). If there has been a very light ephemeral snow fall that melts after only a day or two, only the MCD43A 1-day daily products will capture that snow while the MCD43A standard and 16-day daily products will ignore those observations and only retrieve snow-free albedos. During midwinter days at Fort Peck site, the solar zenith angles at noon can be large and may be around or over 70°, which exceeds the recommended limits of the product.

Fig. 6 shows the comparison among the MCD43A standard, MCD43A 1-day daily and MCD43A 16-day daily albedo with ground measurements. The error bars show the maximum and minimum albedos measured in the field at the various towers during local time 10:30 to 13:30.

All SURFRAD and BSRN sites show good agreement between the various MODIS albedo products and the ground measurements during the height of the growing season. However the MODIS albedo values at the Goodwin Creek, Penn State, and Bondville sites underestimate the tower measurements during the spring and fall seasons. The higher subpixel heterogeneity around the Bondville site, which is surrounded by soybean and corn fields, may cause this seasonal discrepancy (Salomon et al., 2006) and the wet drainage system around the Bondville site also depresses the MODIS albedo. At the Goodwin Creek and Penn State sites, the grassland and agricultural fields where the tower is located are surrounded by mixed forest, which is captured by the coarser MODIS products and results in lower values during the shoulder seasons.

During the dormant snow-free season, the Bondville, Penn State, Sioux Falls and Goodwin Creek stations are particularly heterogeneous (not spatially representative) and show large differences between MODIS albedo and ground measurements in 2004. At the Bondville site, the MCD43A 1-day daily results are close to the ground measurements when the surface is completely covered by snow and therefore is more homogenous (the drainage ditches are frozen and snow-covered). However, the surface is more heterogeneous and the MODIS albedos are about 0.12 lower than the ground measurements at the Bondville site during the dormant snow-free season. MCD43A albedos are lower than the ground measurements at Penn State site in 2004 because of the effect of the nearby forest. The MODIS albedos are about 0.08 lower than the ground measurements during dormant snow-free period. The tower footprint is dominated by bright snow while the MODIS footprint also contains the darker forest land and the MODIS albedos are about 0.17 lower than the ground measurements

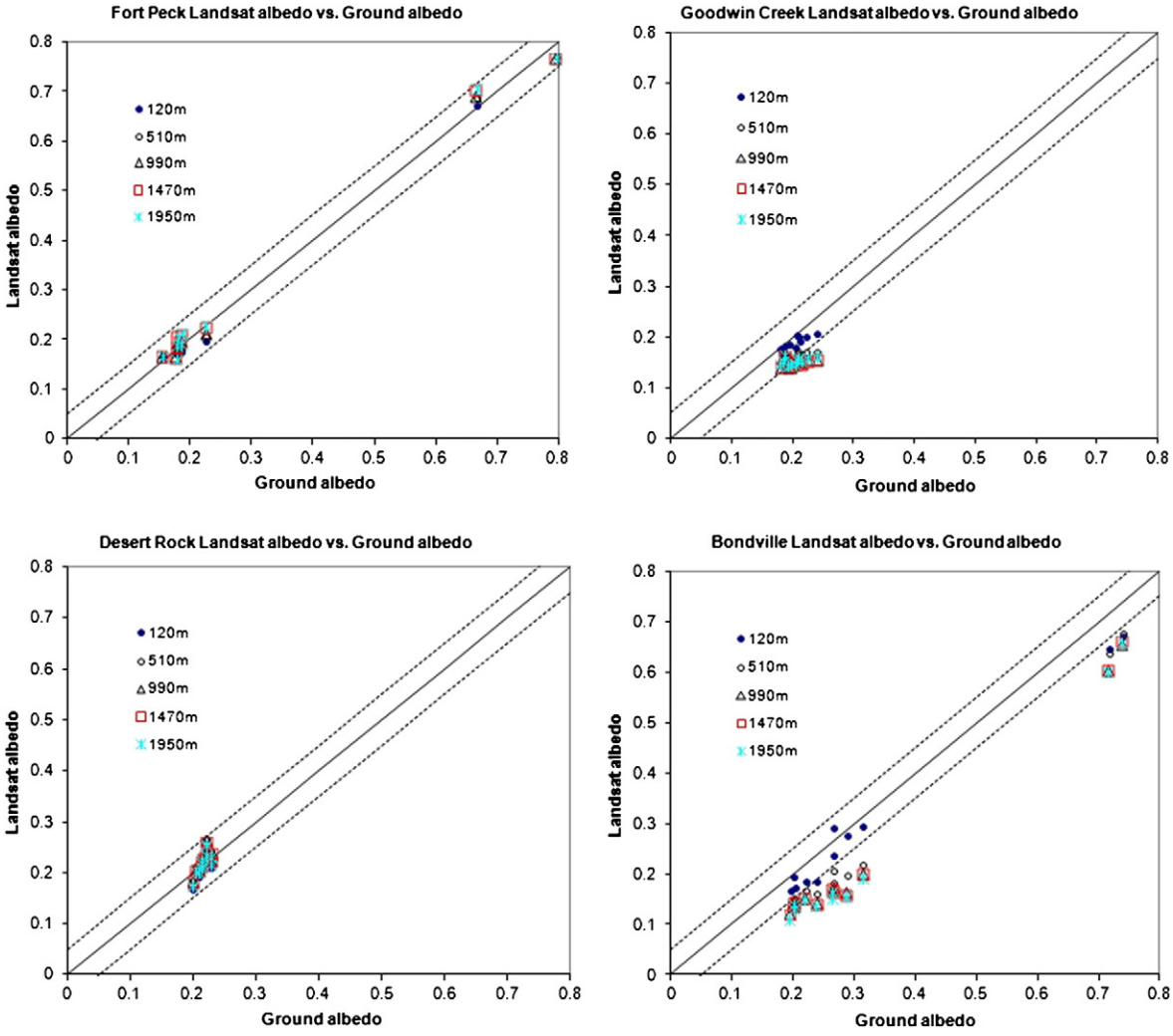

Fig. 7. Scatterplots between the ground albedo and different spatial resolutions of Landsat albedo for Fort Peck (a), Goodwin Creek (b), Desert Rock (c) and Bondville (d) from 2003 to 2009.

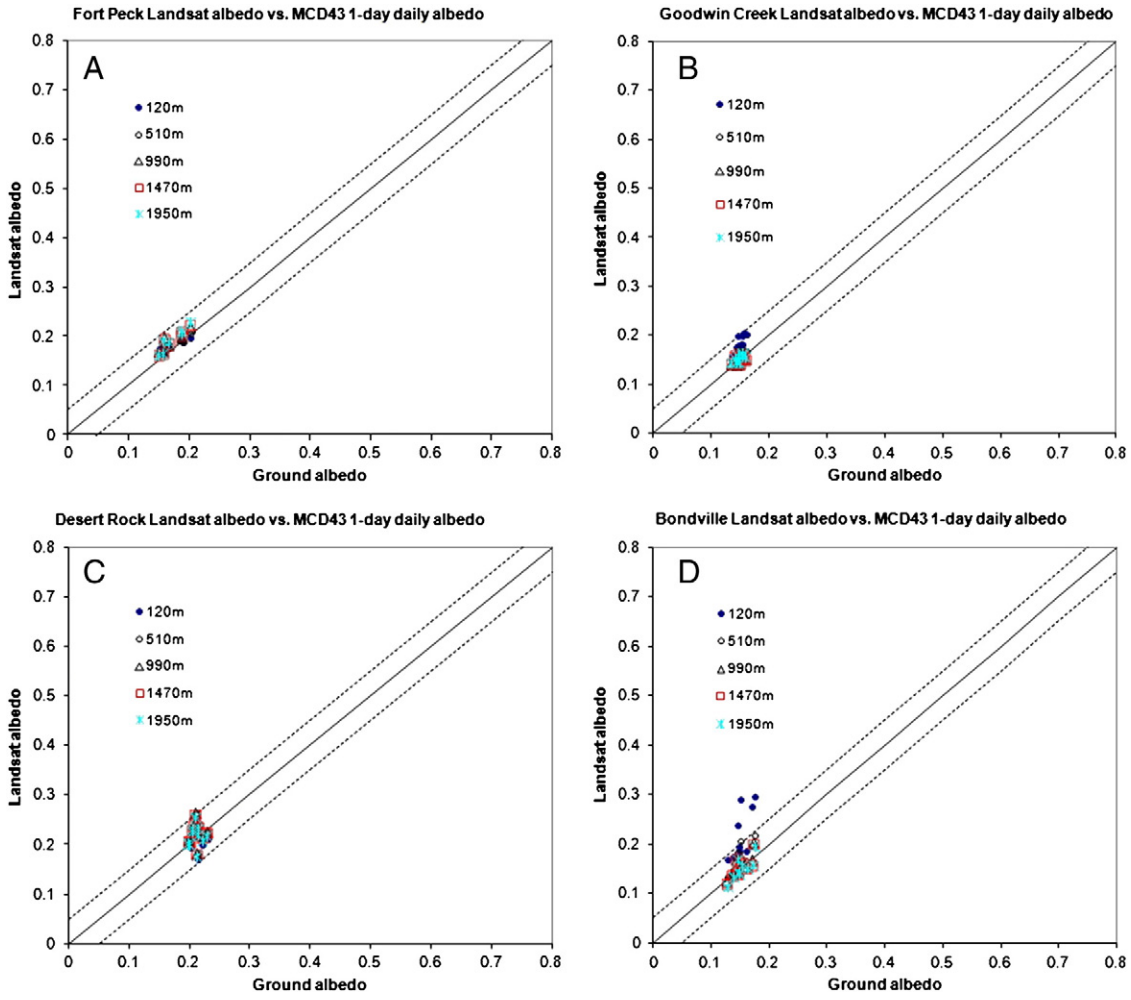

Fig. 8. Scatterplots between the MCD43A 1-day daily albedo and different spatial resolutions of Landsat albedo for Fort Peck (A), Goodwin Creek (B), Desert Rock (C) and Bondville (D) from 2003 to 2009.

during snow-covered period. There is no snow at Goodwin Creek site and the MODIS albedos are about 0.07 lower than the ground measurements during dormant snow-free period where ground measurements are capturing only grassland while MODIS footprint covers some additional forested areas.

The MCD43A 1-day daily albedos are closer to the ground measurements during both the winter dormant and the snow-covered periods at Boulder, Table Mountain, and Fort Peck sites. These sites are all spatially representative (relatively homogeneous). There is no snow throughout the year at the Desert Rock station and the ground albedo agrees with all the MODIS albedo products very well. Over the spatially representative sites of agriculture and grassland, the RMSEs are less than 0.03 during the dormant periods and less than 0.05 during the snow-covered periods for MCD43A 16-day daily, MCD43A 1-day daily and MCD43A standard albedos from 2003 to 2008 (Table 6).

MCD43A 1-day daily, MCD43A 16-day daily and MCD43A standard albedo all also demonstrate relatively good accuracies (RMSE = 0.025 for both full inversions and magnitude inversions) at Howland West

Table 2
Comparative results between the different spatial resolutions of Landsat albedo and ground measurements over eight SURFRAD/BSRN sites from 2003 to 2009.

Study sites	Resolutions									
	120 m		510 m		990 m		1470 m		1950 m	
	Bias	RMSE	Bias	RMSE	Bias	RMSE	Bias	RMSE	Bias	RMSE
Boulder[a]	0.004	0.018	0.017	0.031	0.023	0.037	0.026	0.038	0.026	0.035
Fort Peck	0.003	0.012	0.004	0.015	0.007	0.017	0.010	0.022	0.011	0.023
Goodwin Creek	−0.016	0.019	−0.039	0.042	−0.050	0.053	−0.052	0.055	−0.048	0.051
Sioux Falls	−0.043	0.044	−0.026	0.038	−0.048	0.055	−0.054	0.057	−0.055	0.059
Table Mountain	0.014	0.027	0.027	0.033	0.031	0.036	0.034	0.036	0.035	
	0.012									
Desert Rock	−0.003	0.015	0.012	0.019	0.010	0.018	0.008	0.017	0.004	0.015
Bondville	−0.028	0.038	−0.067	0.069	−0.087	0.089	−0.090	0.093	−0.093	0.096
Penn State	−0.025	0.039	−0.028	0.035	−0.042	0.044	−0.055	0.057	−0.063	0.065

[a] The bias and RMSE with 3810 m aggregated Landsat albedo are 0.025 and 0.038 respectively.

Table 3
Comparative results between the different spatial resolutions of Landsat albedo and MCD43A 1-day daily albedo over eight SURFRAD/BSRN sites from 2003 to 2009.

Study sites	Resolutions									
	120 m		510 m		990 m		1470 m		1950 m	
	Bias	RMSE	Bias	RMSE	Bias	RMSE	Bias	RMSE	Bias	RMSE
Boulder[a]	−0.012	0.028	0.011	0.033	0.017	0.037	0.021	0.037	0.020	0.034
Fort Peck	0.013	0.015	0.016	0.016	0.020	0.019	0.023	0.021	0.024	0.022
Goodwin Creek	0.039	0.038	0.015	0.016	0.005	0.008	0.003	0.007	0.007	0.008
Sioux Falls	0.009	0.024	0.025	0.026	0.003	0.008	−0.002	0.016	−0.004	0.018
Table Mountain	0.012	0.025	0.026	0.031	0.031	0.034	0.034	0.035	0.034	
0.010										
Desert Rock	0.002	0.021	0.017	0.028	0.015	0.027	0.013	0.025	0.009	0.024
Bondville	0.073	0.076	0.025	0.028	0.007	0.014	0.003	0.013	0.000	0.012
Penn State	0.042	0.058	0.039	0.048	0.025	0.029	0.011	0.012	0.004	0.006

[a] The bias and RMSE with 3810 m aggregated Landsat albedo are 0.020 and 0.037 respectively.

site during the snow-covered periods in 2007. During the snow-covered periods in 2008 and 2009 however, the ground albedos are much lower than the MODIS albedos. Ground albedos have values of only about 0.09 while the MODIS albedos values are around 0.14. This occurs because during the snow-covered period, the MODIS pixels contain part of the significantly brighter snow-covered recently harvested areas to the north, while ground data are measured from dense evergreen forest only. At the Howland Larch site in 2008, the MODIS albedos are a little lower than ground measurements because MODIS captures more of the nearby areas of evergreen forest. The differences are still mostly less than 0.05 absolute albedo. The MODIS albedos at Harvard EMS tower agree quite well with the ground measurements. The ground tower footprint evidently captures enough of the same variability as sensed by MODIS pixel. The RMSEs are less than 0.020 during the dormant periods and less than 0.025 during the snow-covered periods for MCD43A 16-day daily, MCD43A 1-day daily, and MCD43A standard albedo at the Howland West Tower and Harvard EMS tower sites in 2007 (Table 6).

For the Howland West site, the snow-covered period is about from DOY 1 to 89 and 340 to 365 in 2007. During 2008, the snow-covered period occurs before DOY 108 and after 353. At the Howland Larch site, the snow-covered period occurs before about DOY 108 in 2008. The Table Mountain site was only covered by snow a few days in 2004. Due to the rapid snowmelt, the change can be 0.17 or more within 3 h. Most MCD43A albedos are within the range of the maximum and minimum ground measurements, however.

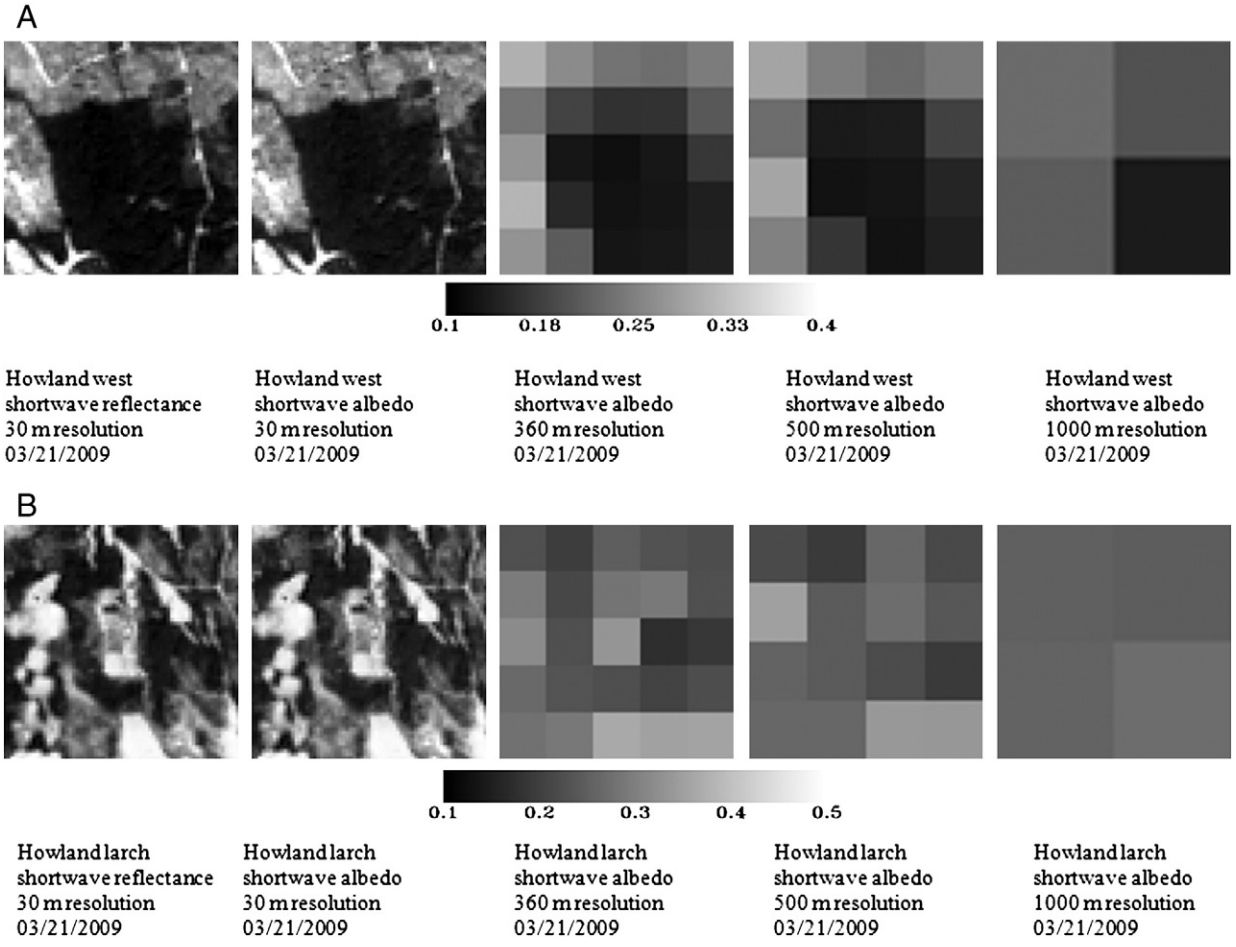

Fig. 9. Different spatial resolutions of Landsat shortwave reflectance and reconstructed albedo for Howland West and Larch sites on 03/21/2009 within a 2 km by 2 km window size.

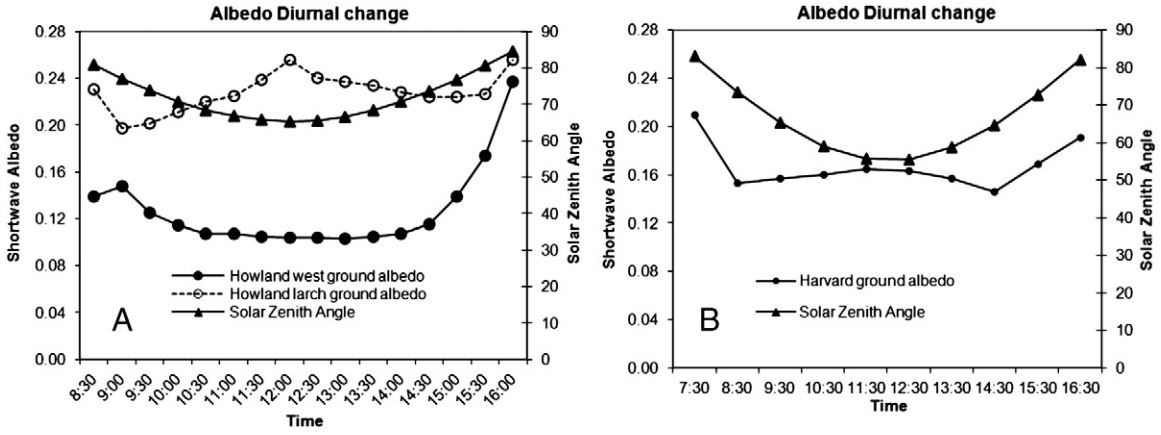

Fig. 10. Diurnal change of Howland West and Larch ground albedo on DOY 20 in 2008 (A) and Harvard ground albedo on DOY 46 in 2007 (B).

4.2.2. Comparison of ground albedo with MODIS and Landsat derived albedo

Ground measurements, Landsat albedo, and MODIS albedo agree well over all spatial resolutions for the spatially representative stations (Table Mountain, Desert Rock, Boulder and Fort Peck) during the dormant periods (Figs. 7 and 8). The 120 m spatial resolution Landsat albedos (which are closest to the 126 m tower footprints) all agree well with ground albedos during all dormant periods even for the highly heterogeneous (spatially non-representative) sites (Tables 2 and 3). The larger spatial scale albedos do show larger discrepancies at the more heterogeneous Penn State, Bondville, Boulder and Sioux Falls sites when they are experiencing partly snow-covered conditions, while still showing good agreement at the representative Fort Peck site under completely snow-covered conditions.

Table 2 provides the bias (Landsat albedo minus ground albedo) and RMSE between different spatial resolutions of aggregated Landsat albedos and the ground albedos during both the dormant and snow-covered periods. The biases for all spatial resolutions are within the range of 0.012 to 0.036 for Table Mountain, 0.004 to 0.026 for Boulder, −0.003 to 0.012 for Desert Rock and 0.003 to 0.011 for Fort Peck. Bondville, Goodwin Creek, Sioux Falls and Penn State sites are more heterogeneous and less spatially representative of the satellite footprints and over these sites, the Landsat albedos are closest to the ground measurements at the 120 m spatial resolution, but these biases increase with the coarser resolution aggregated Landsat albedos (Fig. 7). For example, the biases change from −0.028 (120 m) to −0.093 (at 1950 m) and the RMSE increases from 0.038 to 0.096 at the Bondville site (Table 2).

Table 3 provides the bias and RMSE between different spatial resolutions of Landsat albedo and the MCD43A 1-day daily albedo during the dormant and snow-covered periods. The MODIS and Landsat albedo differences are the least at scales equal to or larger than a 990 m spatial resolution over non-spatially representative sites (Bondville, Goodwin Creek, Sioux Falls and Penn State), but these differences are greatest with the 120 m Landsat albedo (and thus the ground albedo) (Fig. 8). The RMSE between MODIS and Landsat albedo drops from 0.076 (at 120 m) to 0.012 (at 1950 m) at the heterogeneous Bondville site. At the Goodwin Creek, the RMSE decreases from 0.038 (at 120 m) to 0.008 (at 1950 m) and from 0.058 (at 120 m) to 0.006 (at 1950 m) at the Penn State site. The bias and RMSE are very close when the spatial resolutions are coarser than 510 m for these three sites. These findings emphasize that we should not compare the MODIS products to ground measurements directly at the spatially unrepresentative sites. Instead finer spatial resolution satellite products must be used to interconnect them.

Fig. 9 shows the different spatial resolutions of Landsat shortwave reflectance and reconstructed albedo for the Harvard EMS site on 04/28/2006 and Howland West and Larch sites on 03/21/2009 within a 2 km by 2 km window size. The 30 m Landsat albedos within the window capture some bare patches which can be covered by bright snow during the snow-covered period. The Landsat albedos acquired at the Howland Larch site did include some brighter snow-covered components. The albedos vary from 0.1 to about 0.6 during the snow-covered period over Harvard and Howland sites.

Ground measurements vary with the different solar zenith angles observed within a day. At the dense Howland West site, any snow lying on the forest floor is not observed particularly well by the tower albedometer. Therefore the albedo show a typical "U" shape (Fig. 10) throughout the day which is really quite similar with the pattern observed during the growing season (Liu et al., 2009). At the Howland Larch site (where the deciduous foliage has dropped), the albedos are quite high even when the solar zenith angle is low. The shadows the branches are casting on the snow covering the forest floor are smallest at local solar noon and the surface is therefore the brightest. The albedo at local solar noon is 0.035 larger than that observed at 10:30 on DOY 20 in 2008. The Harvard EMS site shows a slight increase surrounding local solar noon because it is a mixed forest with dense deciduous branches and evergreen trees. Only part of the snow signal can still escape the canopy to be observed by the albedometer. This special 3D forest structure increases the difficulty of comparison of ground albedo with satellite albedo. The difference among them would increase if the angular sampling of the input reflectance for the MODIS BRDF/albedo retrieval cannot capture this.

The ground, MCD43A 1-day daily, MCD43A 16-day daily, the standard MCD43A and the Landsat albedos aggregated at different spatial resolutions all agree very well at the spatially representative Harvard EMS tower during late dormant period (Table 4). The difference between the MODIS albedo and the 1950 m aggregated Landsat albedo is largest on DOY 2009080 at the Howland West site, after the largest

Table 4
Comparison of ground albedo with different spatial resolutions of Landsat albedo, MCD43A 1-day daily, MCD43A 16-day daily and MCD43A standard albedo on DOY 2007091, 2008078, and 2009080 for the Howland West and Larch sites and 2006118 for Harvard EMS site.

Site	Harvard EMS site	Howland Larch site	Howland West site	Howland West site	Howland West site
DOY	2006118	2009080	2007091	2008078	2009080
Ground (366 m)	0.115	0.227	0.075	0.086	0.080
Landsat 360 m	0.101	0.339	0.110	0.121	0.117
Landsat 510 m	0.104	0.303	0.110	0.121	0.117
Landsat 990 m	0.108	0.244	0.116	0.132	0.126
Landsat 1470 m	0.111	0.254	0.125	0.174	0.163
Landsat 1950 m	0.111	0.258	0.130	0.141	0.188
MCD43A 1-day daily	0.108	0.194	0.093	0.140	0.135
MCD43A 16-day daily	0.115	0.184	0.104	0.139	0.135
MCD43A standard	0.114	0.186	0.097	0.152	0.137

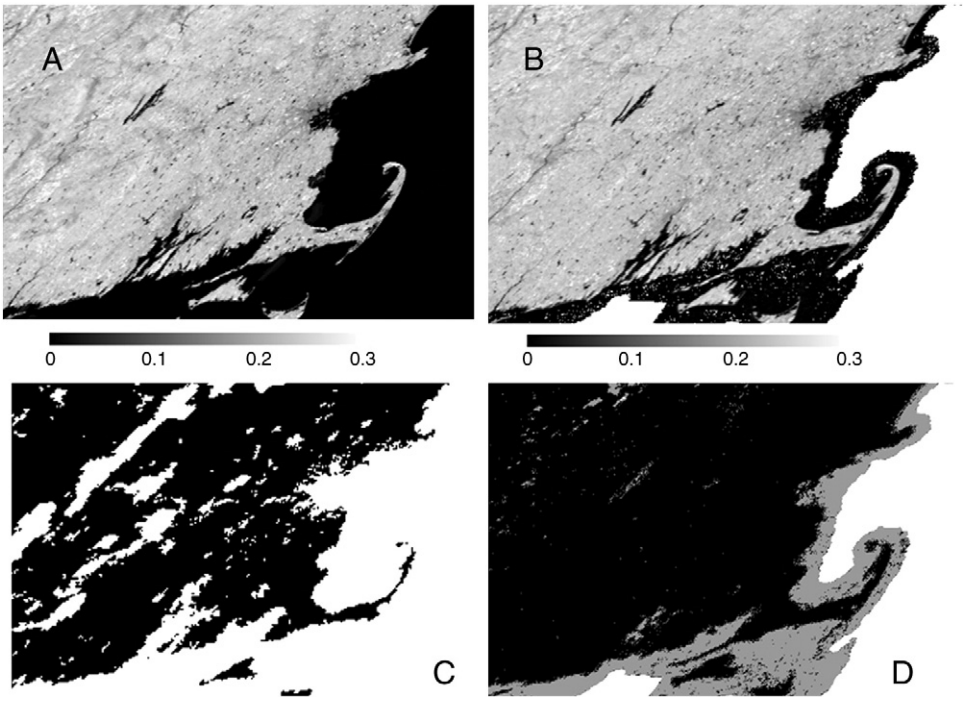

Fig. 11. Observed (A) and predicted (B) reflectance, observations quality flag (C), and MCD43A quality flags (D) used for prediction around Harvard forest over 200 km by 300 km area on DOY 90 in 2006 for NIR band. For MCD43A quality flag, full inversions are in black, magnitude inversions are in gray and filled values are in white. For observations quality flag, clear sky observations over land are in black.

amount of harvesting has occurred. The Landsat albedos are a little larger than the ground measurements at the Howland West site (although the differences are less than 0.037) between the 360 m aggregated Landsat and ground albedos with 366 m footprint. Ground albedos at Howland Larch site are quite close to both the MODIS and Landsat albedos when the spatial resolutions are equal to or larger than 990 m. The bias is less than 0.04. But the Landsat albedos at 360 m and 510 m are much larger than the ground albedo values because the satellite products contain more pure snow contributions. This occurs because the larch trees lie in a relative thin rectangular area. The MCD43A 1-day daily albedo is 0.145 lower than 360 m aggregated Landsat albedo and 0.109 lower than 510 m aggregated Landsat albedo. The MODIS observations at large view zenith angles usually capture more of the surrounding evergreen forests (and also do not capture all the small bright areas of snow).

4.3. Comparison of observed with predicted observations

While comparison of the satellite based products with high quality field data represent a rigorous validation, another internal assessment can be made with the MCD43A product by using the BRDF model retrieved on one day to predict the surface reflectance that will be observed on the next clear day (Schaaf et al., 2002). This method has the added advantage of evaluating both the applicability of the retrieved BRDF model and the quality of the intrinsic albedo derived from it and this method can also be applied to larger regions than just the area surrounding a tower site.

Ten days worth of clear sky observations are selected during January and February 2008 at the Howland West site and used to compare the model predicted reflectance to the observed reflectance. The RMSE is 0.026 between the predicted and observed shortwave reflectance. In

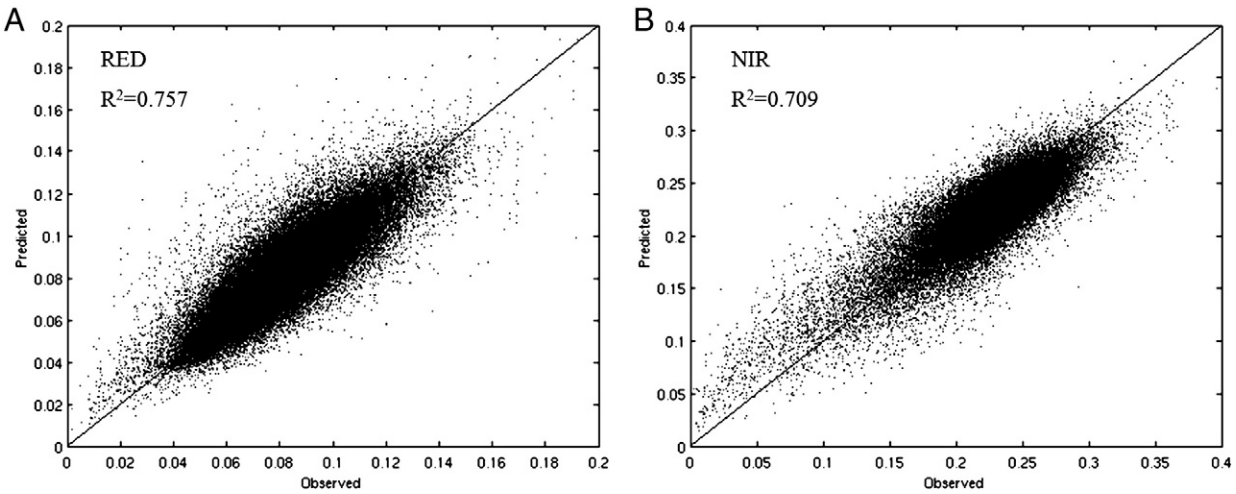

Fig. 12. Scatterplots between observed and predicted reflectance around Harvard forest over 200 km by 300 km area on DOY 90 in 2006 for red band (A) and NIR band (B).

Table 5
Comparative results between predicted reflectance and observed reflectance for a 200 km by 300 km area around Harvard Forest for the red and NIR MODIS bands on DOY 90, 2006.

Inversion types	Number of pixels	Statistics	Red predicted	NIR predicted
All	118,885	Correlation coefficient	0.8702	0.8407
		R^2	0.7570	0.7090
		Bias	−0.0004	−0.0033
		RMSE	0.0094	0.0160
Full inversion	117,966	Correlation coefficient	0.8734	0.8386
		R^2	0.7630	0.7030
		Bias	−0.0005	−0.0033
		RMSE	0.0092	0.0160
Magnitude inversion	919	Correlation coefficient	0.8030	0.8990
		R^2	0.6450	0.8080
		Bias	0.0120	0.0050
		RMSE	0.0230	0.0250

addition to the site single pixel comparison, we also compare the predicted and observed reflectances over a large 200 km by 300 km area in tile h12v04 including Harvard Forest for DOY 90 in 2006 (Figs. 11 and 12). For MCD43A quality flag, full inversions (high quality) are in black, magnitude inversions (poor quality) are in gray and filled values are in white. For observations quality flag, clear sky (cloud-free and low aerosol) observations over land are in the black in Fig. 11. The BRDF parameters were retrieved with the observations from DOY 73 to DOY 88. DOY 89 was not used here because of widespread cloudiness. Predicted reflectances are calculated with the same illumination and viewing angles as the actual observations. The correlation coefficient is 0.87 ($R^2 = 0.76$) for red band and 0.84 (R-square = 0.71) for NIR band over clear sky pixels on land if both full inversion and magnitude inversions are considered. The biases are within 0.012 and RMSE are less than 0.025 for both red and NIR bands of full inversions and magnitude inversions (Table 5). The number of full inversions pixels is 117,966 while there are only 919 pixels of the magnitude inversions. The correlation coefficient of the magnitude inversions for the NIR is actually a little larger than the values achieved from just full inversions. However, the bias and RMSE of the magnitude inversions are all much worse than the full inversions.

5. Conclusions

The MODIS albedo products over dormant and snow-covered periods were evaluated for agriculture/grassland SURFRAD, BSRN sites and evergreen, deciduous, and mixed AmeriFlux forests sites. Finer spatial resolution Landsat data were used in this study to analyze the spatial representativeness of tower measurements and link the different spatial scales of retrieved albedos. MCD43A albedo products match the field measurements quite well during the dormant and snow period at spatially representative sites. However, at non-representative sites (particularly during snow-covered periods), the two albedos can be quite different. The Boulder, Desert Rock, Fort Peck, Table Mountain and Harvard EMS sites are spatially representative during all the seasons. The Bondville, Sioux Falls, Goodwin Creek, Penn State and Howland West sites are more heterogeneous and not spatially representative and Howland Larch site is relative spatially representative during the dormant and snow periods. Nearly all sites are spatially representative during the growing season except Howland West site due to the clear cut. In general the RMSEs are 0.029, 0.028, and 0.030 over spatially representative sites of agriculture/grassland during dormant periods and 0.041, 0.046, and 0.050 during snow-covered periods for MCD43A 1-day daily, MCD43A 16-day daily, and MCD43A standard albedo respectively for both full inversions and magnitude inversions. For forests, the RMSEs are 0.010, 0.020, and 0.011 during dormant period and 0.025, 0.025, and 0.025 during snow-covered period for MCD43A 1-day daily, MCD43A 16-day daily, and MCD43A standard albedo respectively both full inversions and magnitude inversions (Table 6).

Table 6
The accuracy of MCD43A albedo products during dormant and snow period.

Land cover			Agriculture/ grassland		Forest	
Periods			Dormant	Snow-covered	Dormant	Snow-covered
MCD43A 1-day daily albedo	Magnitude inversion	Bias	±0.023	±0.025	±0.001	±0.023
		RMSE	0.029	0.041	0.010	0.025
MCD43A 16-day daily albedo	Full inversion	Bias	±0.023	±0.027	±0.005	±0.005
		RMSE	0.027	0.041	0.010	0.005
	Magnitude inversion	Bias	±0.016	±0.026	±0.006	±0.023
		RMSE	0.028	0.046	0.020	0.025
MCD43A standard albedo	Full inversion	Bias	±0.019	±0.018	±0.001	±0.005
		RMSE	0.025	0.022	0.007	0.005
	Magnitude inversion	Bias	±0.027	±0.030	±0.006	±0.025
		RMSE	0.030	0.050	0.011	0.025

The field measurements (which represent a 126 m footprint from a 10 m tower) for non-spatially representative SURFRAD sites are closest to the 120 m Landsat albedos, but the biases are larger when compared to coarser aggregated Landsat data. Similarly, the MODIS albedos (provided at a 500 m gridded resolution but generally representative of a larger footprint) agree well with the coarser aggregated Landsat albedos, but have a larger difference with the 120 m Landsat albedo (and thus ground albedo).

The diurnal behavior of ground measurements reveals the effects of a multi-layer canopy on any underlying snow. The shadows of trunk and branches on the forest floor decrease with a decrease of solar zenith angle, so more of the understory snow is illuminated under lower solar zenith angle and the albedo measured is larger than that under higher solar zenith angles.

This study demonstrates that the surface spatial representativeness of a ground site must be established before validation if the footprint of the tower measurements is very different from that of the MODIS products. MCD43A 1-day daily product is able to capture the rapid change of albedo during the snow melt period. The ephemeral snow during winter decreases the accuracy of MCD43A 16-day daily and MCD43A standard albedo which assume the land surface status is relatively stable within the 16 days.

Acknowledgments

This research was supported by NASA awards NNX09AL03G, NNX08AE94A, and NNX11AD58G. The MODIS data were obtained from the NASA Distributed Active Archive Centers (DAACs). The Landsat data were obtained from the USGS Earth Resources Observation and Science (EROS) Center.

References

Augustine, J. A., DeLuisi, J., & Long, C. (2000). SURFRAD: A national surface radiation budget network for atmospheric research. *Bulletin of the American Meteorological Society, 81*, 2341–2357. http://dx.doi.org/10.1175/1520-0477.

Barnsley, M. J., Hobson, P. D., Hyman, A. H., Lucht, W., Muller, J. -P., & Strahler, A. H. (2000). Characterizing the spatial variability of broadband albedo in a semidesert environment for MODIS validation. *Remote Sensing of Environment, 74*, 58–68.

Betts, A. K., & Ball, J. H. (1997). Albedo over the boreal forest. *Journal of Geophysical Research — Atmospheres, 102*, 28901–28909.

Bonan, G. B., Chapin, F. S., III, & Thompson, S. L. (1995). Boreal forest and tundra ecosystems as components of the climate system. *Climate Change, 29*, 145–167.

Carroll, S. S., & Cressie, N. (1996). A comparison of geostatistical methodologies used to estimate snow water equivalent. *Water Resources Bulletin, 32*, 267–278.

Chen, Y. M., Liang, S., Wang, J., Kim, H. Y., & Martonchik, J. V. (2008). Validation of MISR land surface broadband albedo. *International Journal of Remote Sensing, 29*, 6971–6983.

Cooper, S. D., Barmuta, L., Sarnelle, O., Kratz, K., & Diehl, S. (1997). Quantifying spatial heterogeneity in streams. *Journal of the North American Benthological Society*, *16*, 174–188.

Davis, J. C. (1986). *Statistics and data analysis in geology*. New York Wiley.

Dickinson, R. E. (1983). Land surface processes and climate–surface albedos and energy balance. *Advances in Geophysics*, *25*, 305–353.

Dickinson, R. E. (1995). Land processes in climate models. *Remote Sensing of Environment*, *51*, 27–38.

Dickinson, R. E., & Hanson, B. (1984). Vegetation-albedo feedbacks. In J. E. Hansen, & T. Takahashi (Eds.), *Climate Processes and Climate Sensitivity*. *Geophysical Monograph Series*, *Vol. 29*. (pp. 180–186). Washington, D.C. AGU. http://dx.doi.org/10.1029/GM029p0180.

Dickinson, R. E., Zhou, L., Tian, Y., Liu, Q., Lavergne, T., Pinty, B., et al. (2008). A three-dimensional analytic model for the scattering of a spherical bush. *Journal of Geophysical Research*, *113*, D20113. http://dx.doi.org/10.1029/2007JD009564.

Dirmeyer, P. A., & Shukla, J. (1994). Albedo as a modulator of climate response to tropical deforestation. *Journal of Geophysical Research*, *99*, 20863–20877.

Disney, M., Lewis, P., Thackrah, G., Quaife, T., & Barnsley, M. (2004). Comparison of MODIS broadband albedo over an agricultural site with ground measurements and values derived from Earth observation data at a range of spatial scales. *International Journal of Remote Sensing*, *25*, 5297–5317.

Fang, H., Liang, S., Chen, M., Walthall, C., & Daughtry, C. (2004). Intercomparison of MISR land surface reflectance and albedo products with ETM+ and MODIS products. *International Journal of Remote Sensing*, *25*(2), 409–422.

Fang, H., Liang, S., Kim, H. Y., Townshend, J. R., Schaaf, C. L., Stralher, A. H., et al. (2007). Developing spatially continuous 1 km surface albedo dataset over North America from Terra MODIS products. *Journal of Geophysical Research — Atmosphere*, *112*. http://dx.doi.org/10.1029/2006JD008377.

Gao, F., Schaaf, C. B., Strahler, A. H., Jin, Y., & Li, X. (2003). Detecting vegetation structure using a kernel-based BRDF model. *Remote Sensing of Environment*, *86*(2), 198–205.

Gao, F., Schaaf, C. B., Strahler, A. H., & Lucht, W. (2001). Using a multi-kernel least variance approach to retrieve and evaluate albedo from limited BRDF observations. *Remote Sensing of Environment*, *76*, 57–66.

Gardner, A. S., & Sharp, M. J. (2010). A review of snow and ice albedo and the development of a new physically based broadband albedo parameterization. *Journal of Geophysical Research*, *115*, F01009. http://dx.doi.org/10.1029/2009JF001444.

Henderson-Sellers, A., & Wilson, M. F. (1983). Surface albedo data for climatic modeling. *Reviews of Geophysics*, *21*, 1743–1778.

Hill, M. J., Averill, C., Jiao, Z., Schaaf, C. B., & Armston, J.D. (2008). Relationship of MISR RPV parameters and MODIS BRDF shape indicators to surface vegetation patterns in an Australian tropical savanna. *Canadian Journal of Remote Sensing*, *34*(Suppl. 2), S247–S267.

Hollinger, D. Y., Ollinger, S. V., Richardson, A.D., Meyers, T. P., & Dail, D. B. (2010). Albedo estimates for land surface models and support for a new paradigm based on foliage nitrogen concentration. *Global Change Biology*, *16*, 696–710.

Isaaks, E. H., & Srivastava, R. M. (1989). *An introduction to applied geostatistics*. New York Oxford University Press.

Jin, Y., Schaaf, C. B., Gao, F., Li, X., Strahler, A. H., Zeng, X., et al. (2002). How does snow impact the albedo of vegetated land surfaces as analyzed with MODIS data? *Geophysical Research Letters*, *29*. http://dx.doi.org/10.1029/2001GL014132.

Jin, Y., Schaaf, C. B., Woodcock, C. E., Gao, F., Li, X., Strahler, A. H., et al. (2003a). Consistency of MODIS surface BRDF/Albedo retrievals: 1. Algorithm performance. *Journal of Geophysical Research*, *108*(D5), 4158. http://dx.doi.org/10.1029/2002JD002803.

Jin, Y., Schaaf, C. B., Woodcock, C. E., Gao, F., Li, X., Strahler, A. H., et al. (2003b). Consistency of MODIS surface BRDF/Albedo retrievals: 2. Validation. *Journal of Geophysical Research*, *108*(D5), 4159. http://dx.doi.org/10.1029/2002JD002804.

Knobelspiesse, K. D., Cairns, B., Schmid, B., Román, O. M., & Schaaf, B. C. (2008). Surface BRDF estimation from an aircraft compared to MODIS and ground estimates at the Southern Great Plains site. *Journal of Geophysical Research*, *113*, D20105.

Koltzow, M. (2007). The effect of a new snow and sea ice albedo scheme on regional climate model simulations. *Journal of Geophysical Research — Atmospheres*, *112*, D07110.

Kotchenova, S. Y., Vermote, E. F., Matarrese, R., & Klemm, F. J. (2006). Validation of a vector version of the 6S radiative transfer code for atmospheric correction of satellite data. Part I: Path radiance. *Applied Optics*, *45*, 6726–6774.

Law, B. E., Falge, E., Gu, L., Baldocchi, D.D., Bakwin, P., Berbigier, P., et al. (2002). Environmental controls over carbon dioxide and water vapor exchange of terrestrial vegetation. *Agricultural and Forest Meteorology*, *113*, 97–120.

Lawrence, P. J., & Chase, T. N. (2007). Representing a new MODIS consistent land surface in the Community Land Model (CLM3.0). *Journal of Geophysical Research*, *112*, G01023.

Lewis, P., & Barnsley, M. J. (1994). Influence of the sky radiance distribution on various formulations of the Earth surface albedo. *Proc. Mesures Physiques et Signatures en Teledetection, Val d'Isere, France, 17–21 January, 1994* (pp. 707–716).

Li, W., Sun, S., Wang, B., & Liu, X. (2009). Numerical simulation of sensitivities of snow melting to spectral composition of the incoming solar radiation. *Advances in Atmospheric Sciences*, *26*, 403–412.

Liang, S. L. (2001). Narrowband to broadband conversions of land surface albedo I. Algorithms. *Remote Sensing of Environment*, *76*, 213–238.

Liang, S., Fang, H., Chen, M., Walthall, C., Daughtry, C., Morisette, J., et al. (2002). Validating MODIS land surface reflectance and albedo products: Methods and preliminary results. *Remote Sensing of Environment*, *83*(1–2), 149–162.

Liang, S., Strahler, A. H., & Walthall, C. (1999). Retrieval of land surface albedo from satellite observations: A simulation study. *Journal of Applied Meteorology*, *38*, 712–725.

Liu, J. C., Schaaf, C. B., Strahler, A. H., Jiao, Z., Shuai, Y., Zhang, Q., et al. (2009). Validation of Moderate Resolution Imaging Spectroradiometer (MODIS) albedo retrieval algorithm: Dependence of albedo on solar zenith angle. *Journal of Geophysical Research — Atmospheres*, *114*, D01106.

Lofgren, B.M. (1995). Surface albedo–climate feedback simulated using two-way coupling. *Journal of Climate*, *8*, 2543–2562.

Lucht, W., Hyman, A. H., Strahler, A. H., Barnsley, M. J., Hobson, P., & Muller, J. P. (2000a). A comparison of satellite-derived spectral albedos to ground-based broadband albedo measurements modeled to satellite spatial scale for a semidesert landscape. *Remote Sensing of Environment*, *74*, 85–98.

Lucht, W., & Lewis, P. (2000). Theoretical noise sensitivity of BRDF and albedo retrieval from the EOS-MODIS and MISR sensors with respect to angular sampling. *International Journal of Remote Sensing*, *21*, 81–98.

Lucht, W., Schaaf, C. B., & Strahler, A. H. (2000b). An algorithm for the retrieval of albedo from space using semiempirical BRDF models. *IEEE Transactions on Geoscience and Remote Sensing*, *38*, 977–998.

Lyons, E. A., Jin, Y., & Randerson, J. T. (2008). Changes in surface albedo after fire in boreal forest ecosystems of interior Alaska assessed using MODIS satellite observations. *Journal of Geophysical Research*, *113*, G02012. http://dx.doi.org/10.1029/2007JG000606.

Marshall, S., Roads, J. O., & Glatzmaier, G. (1994). Snow hydrology in a general circulation model. *Journal of Climate*, *7*, 1251–1269.

Masek, G. J., Vermote, E. F., Saleous, N. E., Wolfe, R., Hall, F. G., Huemmrich, K. F., et al. (2006). A Landsat surface reflectance dataset for North America, 1990–2000. *IEEE Geosience and Remote Sensing Letters*, *3*, 68–72.

Matheron, G. (1963). Principles of geostatistics. *Economic Geology*, *58*, 1246–1266. http://dx.doi.org/10.2113/gsecongeo.58.8.1246.

Michalsky, J. J., Harrison, L. C., & Berkheiser, W. E., III (1995). Cosine response characteristics of some radiometric and photometric sensors. *Solar Energy*, *54*, 397–402.

Molders, N., Luijting, H., & Sassen, K. (2008). Use of atmospheric radiation measurement program data from Barrow, Alaska, for evaluation and development of snow-albedo parameterizations. *Meteorology and Atmospheric Physics*, *99*, 199–219.

Morcrette, J. -L., Barker, H. W., Cole, J. N. S., Iacono, M. J., & Pincus, R. (2008). Impact of a new radiation package, McRad, in the ECMWF integrated forecasting system. *Monthly Weather Review*, *136*, 4773–4798. http://dx.doi.org/10.1175/2008MWR2363.1.

Myhre, G., Kvalevag, M. M., & Schaaf, C. B. (2005). Radiative forcing due to anthropogenic vegetation change based on MODIS surface albedo data set. *Geophysical Research Letters*, *32*, L21410. http://dx.doi.org/10.1029/2005GL024004.

Noreus, J. P., Nyborg, M. R., & Hayling, K. L. (1997). The gravity anomaly field in the Gulf of Bothnia spatially characterized from satellite altimetry and in situ measurements. *Journal of Applied Geophysics*, *37*, 67–84. http://dx.doi.org/10.1016/S0926-9851(97)00007-4.

Ohmura, A., Dutton, E. G., Forgan, B., Frohllch, C., Gllgen, H., Hegner, H., et al. (1998). Baseline Surface Radiation Network (BSRN/WCRP): New precision radiometry for climate research. *Bulletin of the American Meteorological Society*, *79*, 2115–2136.

Oleson, K. W., Bonan, G. B., Schaaf, C. B., Gao, F., Jin, Y., & Strahler, A. (2003). Assessment of global climate model land surface albedo using MODIS data. *Geophysical Research Letters*, *30*, 1443.

Pedersen, C. A., Godtliebsen, F., & Roesch, A.C. (2008). A scale-space approach for detecting significant differences between models and observations using global albedo distributions. *Journal of Geophysical Research*, *113*, D10108.

Pedersen, C. A., Roeckner, E., Luthje, M., & Winther, J. -G. (2009). A new sea ice albedo scheme including melt ponds for ECHAM5 general circulation model. *Journal of Geophysical Research*, *114*, D08101.

Qu, X., & Hall, A. (2006). Assessing snow albedo feedback in simulated climate change. *Journal of Climate*, *19*, 2617–2630.

Roesch, A., Schaaf, C. B., & Gao, F. (2004). Use of Moderate-resolution Imaging Spectroradiometer bidirectional reflectance distribution function products to enhance simulated surface albedos. *Journal of Geophysical Research*, *109*(D12). http://dx.doi.org/10.1029/2004JD004552.

Román, M.O., Schaaf, C. B., Lewis, P., Gao, F., Anderson, G. P., Privette, J. L., et al. (2010). Assessing the coupling between surface albedo derived from MODIS and the fraction of diffuse skylight over spatially-characterized landscapes. *Remote Sensing of Environment*, *114*, 738–760.

Román, M.O., Schaaf, C. B., Woodcock, C. E., Strahler, A. H., Yang, X., Braswell, R. H., et al. (2009). The MODIS (Collection V005) BRDF/albedo product: Assessment of spatial representativeness over forested landscapes. *Remote Sensing of Environment*, *113*, 2476–2498.

Roy, D. P., Lewis, P., Schaaf, C. B., Devadiga, S., & Boschetti, L. (2006). The global impact of clouds on the production of MODIS bidirectional reflectance model-based composites for terrestrial monitoring. *IEEE Geoscience and Remote Sensing Letters*, *3*, 4.

Running, S. W., Baldocchi, D.D., Turner, D. P., Gower, S. T., Bakwin, P.S., & Hibbard, K. A. (1999). A global terrestrial monitoring network integrating tower fluxes, flask sampling, ecosystem modeling and EOS satellite data. *Remote Sensing of Environment*, *70*, 108–127.

Rutter, N., Essery, R., Pomeroy, J., Altimir, N., Andreadis, K., Baker, I., et al. (2009). Evaluation of forest snow processes models (SnowMIP2). *Journal of Geophysical Research*, *114*, D06111.

Salomon, J. G., Schaaf, C. B., Strahler, A. H., Gao, F., & Jin, Y. (2006). Validation of the MODIS bidirectional reflectance distribution function and albedo retrievals using combined observations from the Aqua and Terra platforms. *IEEE Transactions on Geoscience and Remote Sensing*, *44*, 1555–1565.

Samain, O., Kergoat, L., Hiernaux, P., Guichard, F., Mougin, E., Timouk, F., et al. (2008). Analysis of the in-situ and MODIS albedo variability at multiple time scales in the Sahel. *Journal of Geophysical Research*, *113*, D14119. http://dx.doi.org/10.1029/2007JD009174.

Schaaf, C. B., Gao, F., Strahler, A. H., Lucht, W., Li, X., Tsang, T., et al. (2002). First operational BRDF, albedo, nadir reflectance products from MODIS. *Remote Sensing of Environment*, *83*, 135–148.

Schaaf, C. L., Martonchik, J., Pinty, B., Govaerts, Y., Gao, F., Lattanzio, A., et al. (2008). Retrieval of surface albedo from satellite sensors. In S. Liang (Ed.), *Advances in land remote sensing: System, modeling, inversion and application* (pp. 219–243). Springer, 978-1-4020-6449-4.

Schaaf, C. B., Wang, Z., & Strahler, A. H. (2011a). Commentary on Wang and Zender — MODIS snow albedo bias at high solar zenith angles relative to theory and to in situ observations in Greenland. *Remote Sensing of Environment*, *115*, 1296–1300.

Schaaf, C. L. B., Liu, J., Gao, F., & Strahler, A. H. (2011b). MODIS albedo and reflectance anisotropy products from Aqua and Terra. In B. Ramachandran, C. Justice, & M. Abrams (Eds.), *Land remote sensing and global environmental change: NASA's Earth observing system and the science of ASTER and MODIS. Remote Sensing and Digital Image Processing Series*, *Vol. 11*, . Springer-Verlag (873 pp.).

Shuai, Y. (2010). *Tracking daily land surface albedo and reflectance anisotropy with Moderate-resolution Imaging Spectroradiometer (MODIS)*. Dissertation for Doctor of Philosophy. Boston University.

Shuai, Y., Masek, J. G., Gao, F., & Schaaf, C. B. (2011). An algorithm for the retrieval of 30-m snow-free albedo from MODIS BRDF and Landsat surface reflectance. *Remote Sensing of Environment*, *115*, 2204–2216.

Shuai, Y., Schaaf, C. B., Strahler, A. H., Liu, J., & Jiao, Z. (2008). Quality assessment of BRDF/albedo retrievals in MODIS operational system. *Geophysical Research Letters*, *35*, L05407. http://dx.doi.org/10.1029/2007GL032568.

Stone, R. S., Anderson, G. P., Shettle, E. P., Andrews, E., & Loukachine, K. (2008). Radiative impact of boreal smoke in the Arctic: Observed and modeled. *Journal of Geophysical Research*, *113*(D14S16). http://dx.doi.org/10.1029/2007JD009657.

Stroeve, J., Box, J. E., Gao, F., Liang, S., Nolin, A., & Schaaf, C. (2005). Accuracy assessment of the MODIS 16-day albedo product for snow: Comparisons with Greenland in situ measurements. *Remote Sensing of Environment*, *94*, 46–60.

Susaki, J., Yasuoka, Y., Kajiwara, K., Honda, Y., & Hara, K. (2007). Validation of MODIS albedo products of paddy fields in Japan. *IEEE Transactions on Geoscience and Remote Sensing*, *45*, 206–217.

Tan, B., Woodcock, C. E., Hu, J., Zhang, P., Ozdogan, M., Huang, D., et al. (2006). The impact of gridding artifacts on the local spatial properties of MODIS data: Implications for validation, compositing, and band-to-band registration across resolutions. *Remote Sensing of Environment*, *105*, 98–114.

Thomas, G., & Rowntree, P. R. (1992). The boreal forests and climate. *Quarterly Journal of the Royal Meteorological Society*, *118*, 469–497.

Thompson, M., Adams, D., & Johnson, K. N. (2009). The albedo effect and forest carbon offset design. *Journal of Forestry*, *107*, 425–431.

Tian, Y., Dickinson, R. E., Zhou, L., Myneni, R. B., Friedl, M., Schaaf, C. B., et al. (2004). Land boundary conditions from MODIS data and consequences for the albedo of a climate model. *Geophysical Research Letters*, *31*. http://dx.doi.org/10.1029/2003GL019104.

Vermote, E. F., El Saleous, N., Justice, C. O., Kaufman, Y. J., Privette, J. L., Remer, L., et al. (1997). Atmospheric correction of visible to middle infrared EOS-MODIS data over land surfaces: Background, operational algorithm, and validation. *Journal of Geophysical Research*, *102*, 17131–17141.

Viterbo, P., & Betts, A. K. (1999). Impact on ECMWF forecasts of changes to the albedo of the boreal forests in the presence of snow. *Journal of Geophysical Research*, *104*, 27803–27810.

Wang, Z., Barlage, M., Zeng, X. B., Dickinson, R. E., & Schaaf, C. B. (2005). The solar zenith angle dependence of desert albedo. *Geophysical Research Letters*, *32*(5), L05403.

Wang, K. C., Liu, J. M., Zhou, X. J., Sparrow, M., Ma, M., Sun, Z., et al. (2004). Validation of the MODIS global land surface albedo product using ground measurements in a semidesert region on the Tibetan Plateau. *Journal of Geophysical Research*, *109*, D05107.

Wang, Z., Schaaf, C. B., Chopping, M. J., Strahler, A. H., Wang, J., Román, M.O., et al. (2012). Evaluation of Moderate-resolution Imaging Spectroradiometer (MODIS) snow albedo product (MCD43A) over tundra. *Remote Sensing of Environment*, *117*, 264–280.

Wanner, W., Strahler, A. H., Hu, B., Lewis, P., Muller, J. -P., Li, X., et al. (1997). Global retrieval of bidirectional reflectance and albedo over land from EOS MODIS and MISR data: Theory and algorithm. *Journal of Geophysical Research*, *102*, 17143–17162.

Wei, X., Hahmann, A., Dickinson, R. E., Liang, Z. -L., Zeng, X., Schaudt, K., et al. (2001). Comparison of albedos computed by land surface models and evaluation against remotely sensed data. *Journal of Geophysical Research*, *D-106*(20), 687–20702.

Wolfe, R. E., Roy, D. P., & Vermote, E. (1998). MODIS land data storage, gridding, and compositing methodology: Level 2 grid. *IEEE Transactions on Geoscience and Remote Sensing*, *36*, 1324–1338.

Woodcock, C. E., Strahler, A. H., & Jupp, D. L. B. (1988a). The use of variograms in remote sensing: I. Scene models and simulated images. *Remote Sensing of Environment*, *25*, 323–348.

Woodcock, C. E., Strahler, A. H., & Jupp, D. L. B. (1988b). The use of variograms in remote sensing: II. Real digital images. *Remote Sensing of Environment*, *25*, 349–379.

Wyser, K., Jones, C. G., Du, P., Girard, E., Willen, U., Cassano, J., et al. (2007). An evaluation of Arctic cloud and radiation processes during the SHEBA year: Simulation results from eight Arctic regional climate models. *Climate Dynamics*, *30*, 203–223.

Zhou, L., Dickinson, R. E., Tian, Y., Zeng, X., Dai, Y., Yang, Z. -L., et al. (2003). Comparison of seasonal and spatial variations of albedos from Moderate-resolution Imaging Spectroradiometer (MODIS) and common land model. *Journal of Geophysical Research*, *108*(D15), 4488. http://dx.doi.org/10.1029/2002JD003326.